THE PRODUCTION AND ANALYSIS OF MICROCELLULAR FOAM

by

JANE ELLEN MARTINI

A.B., Bryn Mawr College
(1975)

SUBMITTED IN PARTIAL FULFILLMENT
OF THE REQUIREMENTS FOR THE
DEGREE OF

MASTER OF SCIENCE
IN
MECHANICAL ENGINEERING

at the

MASSACHUSETTS INSTITUTE OF TECHNOLOGY

January 1981

Signature of Author _____

Jane Ellen Martini
Department of Mechanical Engineering

Certified by _____

Nam P. Suh
Professor of Mechanical Engineering
Thesis Supervisor

Accepted by _____

Warren M. Rohsenow
Chairman, Department Committee on Graduate Students

THE PRODUCTION AND ANALYSIS OF MICROCELLULAR FOAM

by

JANE ELLEN MARTINI

Abstract

A method for producing microcellular thermoplastic foam (cell diameter 2 to 10 μ) is described. The material produced exhibits tensile strengths superior to those of conventional foam. Unfortunately, the cycle times are too long for commercial application. To gain insight into the design of a more feasible process, the formation and growth of foam was analyzed theoretically. The nucleation rate was predicted by classical nucleation theory applied to a matrix supersaturated with gas. Growth of the cells by diffusion and matrix relaxation was estimated and the size of the cells determined as a function of time.

TABLE OF CONTENTS

"Lions, and tigers and bears- Oh my!"

-to the Lion.

ACKNOWLEDGMENTS

It seems that I have been working toward this thesis for years, and by now it has become my daily companion. There are many, many people who have contributed to its final conclusion; I thank them each and every one.

First of all, I must mention all of the people in Building 35. It is a rare opportunity to have such coworkers -- and friends. At the heart of the laboratory are Ralph and Andy who patiently taught me to use -- not abuse -- the shop. John Ford and Fred Cote were forever lending a helpful hand, and Bob Kane would inevitably come up with a suggestion just slightly better than mine. A big thanks goes to Rich Okine who had the thankless task of trying to guide me, and a colossal thanks to Frank Waldman. If Frank had not helped me, this thesis would probably have taken several years longer! I also thank the people at Kodak and the other members of the Polymer Processing Program for their encouragement, helpful criticism and insights. I thank, too, the 2.30 lab groups, who helped me take reams of data, and all of the people in the SIPB office. The world revolving around Building 35 has become a beloved place. I would not have encountered these people, though, without parents who taught me to reach for my goals. A big hug to them!

But the man who was key to this achievement was Professor Suh. He had the courage to grapple with my mind and motivation, and in doing so, taught me to take pride in my work and have confidence. For the first time in my life, he gave me what I desperately needed -- a mentor.

- 9 -

LIST OF FIGURES

Page

NOMENCLATURE

a = half length of unit cube in Appendix B

A_λ = expansion coefficients for series solution to diffusion equation

Co = initial concentration of gas in the matrix

D = energy stored in elastic deformation

$\mathcal{D}$ = diffusion rate

E = dynamic modulus

$\underline{E}$ = energy stored in the system

E_s = internal energy of solution + elastic deformational energy + surface energy

f = distribution of nucleii sizes

G = Gibb's free energy

ΔG = change in Gibb's free energy

Gg = Gibb's free energy of the gas in the cell

G_s = Gibb's free energy of the polymer-gas solution

J = rate of cell nucleation

k = solubility of gas in matrix

$|\ell|$ = mean jump length between equilibrium positions for gas molecules

n_b = number of moles of gas in bubble

n_i = number of moles of ith component

P = pressure

P = parchor value

$P_b = P_b$ = pressure in the bubble

Q = quantity of heat

dQ = differential quantity of heat

R = radius of the bubble at any time

R = universal gas constant

r_d = radius of the region depleted of gas during nucleation

S = surface energy

$\underline{S}$ = entropy

$S(\eta)$ = surface area of a cell

T = temperature

t = time

U = internal energy

V = volume

V_o = volume of matrix which supplies gas for nucleation

V_b = volume of bubble

W = work

Z = Zeldovich factor

β = rate at which gas molecules strike a unit surface

γ = surface energy coefficient

$\underline{\gamma}$ = rate at which gas molecules are emitted from a unit surface

E_{ij} = strain along the ith face of control cube in j^{th} direction

η = size of a cluster of gas molecules

λ = eigenvalues for characteristic diffusion equation

μ = chemical potential

μ^o = chemical potential at reference temperature

μ^* = chemical potential of the pure component

μ_g = chemical potential of gas

μ_i = chemical potential of ith component

V = molecular volume

ρ = actual density

$\underline{\rho}$ = relative density (of tensile specimen)

ρ_m = density of matrix

δ_{ij} = stress along the ith face of control cube in j^{th} direction

X = concentration of gas

FIGURE I-1 MICROGRAPH OF MICROCELLULAR FOAM

FIGURE I-I MICROGRAPH OF MICROCELLULAR FOAM

I. INTRODUCTION

As the price of petroleum rises, so does the price of plastic.
Currently, for high volume plastic parts, the material accounts for about
60% of the total cost (Hardenburg, 1980). In an effort to reduce the
plastic required for a part, a novel foaming method has been developed.
The process will be discussed in greater detail later. Basically, thermo-
plastic sheet is supersaturated with gas, then heated above its glass
transition temperature (T_g). Once the plastic has softened sufficiently,
it will foam. The resulting material is microcellular (with cells about
2 to 10 μ in diameter) and exhibits tensile strengths superior to those
of conventional foams. Whereas the strength of conventional foam drops
to about 1/5 that of the parent material (Throne, 1979), the strength of
this foam does not drop more than its reduction in density. At 90% of
the parent density, this foam still exhibits 90% of the parent strength,
more than four times that of conventional foam.

The microcellular foam shows some other interesting qualities. The
cells are locally uniform, although those in the center are generally
larger than the ones near the surface. The surface itself is composed
of a thin unfoamed skin. This skin probably results from the gas
diffusing out through the surface rather than forming bubbles. Because
of the skin, the foam has excellent surface characteristics. In fact,
by pressing it against a polished plate just after foaming (while it is

still near T_g), the surface can be made to shine. Since it is not porous, the surface can be printed and decorated by most of the same techniques that are used on the parent material.

In this work, only impact polystyrene was foamed and tested qualitatively. However, crystal grade polystyrene and polycarbonate have also been foamed by this method using N_2 gas. As long as the solubility of the gas in the chosen plastic is high enough, all thermoplastics should be amenable to this process. Whether or not the foam produced will be microcellular depends on many factors.

Adequate strength and lower cost make microcellular foam attractive for many items from calculator housings to tape dispensers. The material is well suited for many packaging applications. Its reduced density may make it useful for airplane or automobile interiors, and perhaps even boat hulls. Measurements have not yet been made of the insulating capabilities of this foam, but it may also have potential as a novel building material. Since this foam is attractive for commercial applications, an obvious question to ask is "Can parts be manufactured from it readily?" The answer to this is "Not yet."

Unfortunately, the current methods of manufacturing foam parts are not ideal. Cycle times are long, and expansion of the foam is often limited by the mold, which results in large cell sizes.

Foamed thermoplastic has existed since the 1940's (Benning, 1969). Most of it is made either from pellets copolymerized with a volitile gas or with chemical or physical blowing agents. Excellent reviews of non-proprietary processes are available (Benning, 1969), (Moiseyev, 1960),

(Throne, 1979), (Hansen, 1962), (Frisch and Sauders, 1973). There has
been quite a bit of work done to minimize cell size and make it uniform.
Generally, this involves the use of nucleating agents, of which there
are several categories:

(a) Fine-sized materials insoluble in the reins.

(b) Chemical agents that react exothermically to produce
    "hot spots".

(c) Chemical reactants which release gas.

(d) Additives that partially destroy the cohesive forces
    between the molecules (Benning, 1969).

Reported cell sizes, however, rarely fall below 0.001 in diameter. One
exception is an open-celled polyolefin with μ diameter cells (Accural,
produced by Armak, Inc.) reported by Worthy (1978).

There are three factors particular to foam which profoundly affect
its manufacturability:

(1) Foam is not thermally stable. Once an article has been
    foamed, it cannot be raised far above its glass transition
    temperature without affecting foam morphology. Thus, making
    major structural changes to the part once it had been foamed
    can pose difficulties. The temperature sensitivity may have
    assets, however, since the material can be returned to its
    unfoamed state by placing it under high temperature when it is
    above T_g. Under these conditions, gas is reabsorbed into
    the polymer.

(2) When an article is foamed, it expands. It is difficult to

maintain critical dimensions through a free expansion process. However, if foam growth is limited, pressure is exerted on the melt which, in turn, causes the gas supersaturation to de- crease. As will be shown later, the amount of supersatura- tion strongly influences cell size.

(3) Heat transfer into and out of the foam is slow. If any process demands large changes in termperature, the cycle times will be long. For the same reason, the surface can be heated quickly without changing the temperature of the core. Thus, surface modifications may be made without distorting the part.

These characteristics are not peculiar to microcellular foam; they are common to foams in general. The manufacturing methods used for conven- tionally foamed parts must cope with these factors. To avoid making major structural changes in a foamed part, the material is often foamed directly into the final shape. Proper dimensions are usually insured by limiting foam growth. For example, foamed parts can be injection molded by expanding ("cracking") the mold to allow for foam growth. The dimensions of the part can be controlled by limiting the mold expansion. Polystyrene foam cups are often made from pentane-filled beads. The beads are poured into a mold and heated. They expand until the mold is filled.

Many of these problems may arise because process designs have adhered to the traditional notions of using molds to form parts. The MIT-Industry Polymer Processing Program   is currently developing a method for forming parts sequentially, much as sheet metal is formed.

This method may be ideally suited for production of parts made from foam, since it can accommodate all three requirements. The gross aspects of the part may be formed before or as the part is foamed. The part may be allowed to foam freely, without regard to dimensional accuracy. The final dimensions may be brought within tolerance by surface modifications.

Regretfully, the sequential forming of microcellular parts is not yet a reality. The current foaming method still poses a severe handicap. The gas is introduced into the plastic by diffusion at room temperature, causing cycle times of about one day. Even raising the temperature during diffusion only reduces the cycle time to hours, which is impractical for commercial applications. It appears that gas must be introduced by a different method.

To make intelligent guesses about how to modify the process to shorten the cycle time, but still produce acceptable foam, it is necessary to understand which aspects of the current process are responsible for the observed morphology. The remainder of the efforts presented here are aimed at that goal. First, tests were made on the effects of changing various process parameters on tensile strength. From this data, the most favorable morphology could be determined. Then the theory of foam nucleation and growth was examined to determine the phenomena responsible for creating such foam. Finally, recommendations are made for modifications to the foaming process. Before launching into these discussions, however, the process itself will be presented in greater detail, and descriptions will be made of other experimental procedures used in this investigation.

II. EXPERIMENTAL PROCEDURES

The following procedures were used to make and test microcellular foam.

A. Foaming Process

Precision extruded, 50 mil thick, impact grade polystyrene sheet (Monsanto, high impact, Kodak Roll #684-1, REX #3222) was placed in a pressure chamber at room temperature. After the plastic had resided in the chamber for the desired length of time, it was removed and heated above Tg in an oven. To keep the delay constant, 6 minutes was allowed between removal from the pressure chamber and insertion in the oven.

The pressure chamber was 3-1/2 in (3" id) cylindrical tube of stainless steel which was capped at both ends. To allow access to the inside of the chamber, one of the caps was sealed with an O-ring and threaded tightening collar. The chamber was fitted with a gas-release valve (needle type), and inlet hose. The inlet hose was steel mesh shrouded and rated for 1000 psi. The chamber was also equipped with a 700 psi burst disk. Gas was supplied to the chamber from a cylinder through a high pressure two-stage regulator (Harris #IC3 with Matheson gauges P/N 63-3143 and PN 63-3133). Since there was no gas flow once the system was sealed, it was assumed that the pressure within the chamber was the same as that set on the regulator. Different gases could be used by changing the cylinder and adapting the regulator.

The oven was constructed of two horizontal 1/4" thick aluminum plates, 14" wide by 22" long. They were held apart 1/4" by rectangular aluminum stock inserted between them along the sides. The oven was

closed by an aluminum flange on the back side, but the front was left open so the plastic sheet could be inserted. This construction avoided the large temperature drops which can occur in conventional ovens when the door is opened. Since the oven chamber was only 1/4" high and since the other three sides were closed, the temperature was not lowered significantly by having the front open. Heat was supplied to the oven by a Chromalex barrel heater (PHD 10S, 120 V, 1000 W, R47), which was wrapped around the outsides of the plates (see Figure II-2a). To prevent edge effects, insulation was installed between the heater and the edge of the plates. A West time proportioning temperature controller (Model 802) was used with an iron-constantan thermocouple to regulate the temperature. With this arrangement, a constant temperature was maintained within 1.5°F in the 12" X 6" region shown in Figure II-2b.

For the variable temperature tests which will be discussed later, the barrel heater was removed, and strip heaters placed on the top and bottom plates at either side. These were set at different temperatures and controlled separately. A series of 5 thermocouples installed between the two heaters showed that the temperature varied linearly with distance. The oven plates were uninsulated for the constant temperature tests (to prevent damage to the barrel heater) and insulated with fiberglass wool for the variable temperature tests. To facilitate moving the plastic in and out of the oven, the samples were placed between two .02 in highly polished aluminum sheets. These could slide easily in and out of the oven. Mold release (4 Release Agent, Contour Chemical Co., Woburn, Mass.) was sprayed on the sheets to prevent the

plastic from sticking and buckling as it expanded.

B. Variation of Process Parameters

To gain insight into the phenomena involved in the formation of foam observations were made of the effects of changing various process parameters on the morphology and strength of the foam produced.

a) Foaming at Differing Temperatures

Ten samples 3.8 cm X 30.5 cm (1-1/2" X 12") were put together in the pressure chamber with (350 psi) N_2 gas for 24 hours. Then, after 6 minutes delay, they were placed side by side in the variable temperature oven described earlier for 7.5 minutes. The oven temperature varied linearly from 88°C (190°F) to 116°C (240°C). The foaming temperature was considered to be the average across any given sample.

b) Foaming for Varying Lengths of Time

Ten 7.6 cm X 15.2 cm (3" X 6") samples were placed in the pressure chamber with N_2 gas at 350 psi. They were removed after 24 hours and, after 6 minutes delay, placed in the oven at 104°C (220°F). Two samples were removed after each: 3 min; 5 min; 7.5 min; 10 mins and 15 mins.

c) Varying Durations of Pressurization and Gas Type

Two 7.6 cm X 15.2 cm (3" X 6") samples were placed in the pressure chamber with N_2 gas for 3 hrs at (350 psi). They were removed and after a 6 min delay, put in the oven at 105°C (220°F) for 7.5 mins. The process was repeated for various chamber residence times up to 116 hrs and with N_2, CO_2 and the gas.

insulation

barrel heater

insulation

opening to oven

(a)

outline of barrel heater

constant temperature area

Top View

(b)

FIGURE II-1 CONSTANT TEMPERATURE OVEN

FIGURE II-2 PRESSURE CHAMBER

FIGURE II-2 PRESSURE CHAMBER

FIGURE II-3 MEASUREMENT OF CELL DIAMETER

C.   Characterization of Foam Morphology

The foams were characterized by their cell size distribution and density.

a) Cell Size Distribution

A scanning electron microscopy was used to determine cell size distribution. The foam was fractured by bending it sharply. It was mounted on end in a holder (beeswax seemed to be a successful mounting medium), and sputtered with gold to form a conductive surface. The sample was then observed with an electron microscope. Micrographs were made of regions of the mid-thickness of the sample. The cell size distributions were found by measuring the diameter of each cell in the lower right quadrant of the micrograph, then plotting the number of cells in each size range. If the cells were not sperical, the measurement was made 45" to the major and minor axies, as shown in Figure II-3. It was assumed that the material fractured through the center of the cells.

b) Density Measurements

Since some of the foams were quite light, it was difficult to use the available density measurement system based on fluids. However, the tensile test specimens were all machined from the same template, so relative density could be found with reasonable reliability by weighing the test specimens and dividing by their thickness. Call this quantity ρ. Changes in thickness across the sample were generally negligible and even in extreme cases less than 2%. The actual density can be found by multiplying the density of the parent material by the ratio of ρ foam

to ρ unfoamed.

$$\rho \text{ foamed} \;=\; \rho \text{ unfoamed} \;\; \frac{\rho \text{ foam}}{\rho \text{ unfoamed}}$$

D. Determination of Tensile Strength

Tensile tests were made in accordance with ASTM specification D 638 (1979, Part 35). The tests were done on Type IV (4.5 in long) specimens. See Figure II.4 for dimensions. They were pulled on an Instron (model 1125) fitted with a D-cell at a rate of .2in/min at room temperature. The thickness of the samples were measured with a 1 in micrometer before they were pulled.

III. STRENGTH OF FOAMS

To determine which factors contribute to the strength of micro-cellular foams, tensile strengths have been measured for foams produced under a variety of processing conditions. Due to limitations in the amount of material available, each experiment was done once, and was not repeated. The results are shown here to give an indication of the trends exhibited. They should be repeated several times to estimate and improve accuracy.

A.   The Effect of Changing Gas Concentration

To attain variation in the gas concentration in the polymer, the material was left in the pressure chamber for various lengths of time (see Chapter II for a description of the process and the experimental procedures). Cell size is plotted against concentration (or time in the pressure chamber) in Figure III-1, and the strength/density ratio is plotted against time in the pressure chamber in Figure III-2. Figure III-3 suggests that larger celled foams are weaker. The primary recommendation for further improvement in foam strength, therefore, is to reduce the cell size even more. As concentration increases, density decreases (Figure III-4). The strength/density ratio is affected by a trade-off of density with cell size. Although a trend between the ratio and concentration is not apparent from the data shown in Figure III-5 it should be noted that the ratio is greater than that for the parent material. Here, especially, the experiments should be repeated to clarify this

FIGURE III-1 CELL SIZE VS. GAS CONCENTRATION

FIGURE III-2 STRENGTH/DENSITY VS. PRESSURE CHAMBER TIME

FIGURE III-3 STRENGTH Vs, CELL SIZE

FIGURE III-4 DENSITY VS. GAS CONCENTRATION

FIGURE III-5 STRENGTH/DENSITY VS. CELL SIZE

data since it will point to an ideal concentration.

B.   The Effect of Changing Foaming Temperature

As the temperature at which the foaming takes place increases, the
density decreases (Figure III-6), the cell size increases (Figure III-7)
and the strength decreases (Figure III-8). Discussion of the reasons for
this are found in Chapter V, Section A.

C.   The Effect of Changing Foaming Time

The data, shown in Figure III-9, has so much scatter that trends of
cell size versus oven time are not distinguishable. From work described
later (Chapter IV, Section C), the cells should be expected to grow about
3% over the period from 3 to 15 minutes (calculated from the graph
IV-21). The strength of the plastic, however, does decrease with the
length of time the plastic is left in the oven (see Figures III-10 and
III-11). It is believed that this reduction in strength reflects the
loss of orientation imposed around the cell by nucleation and diffusional
growth.

FIGURE III-6 DENSITY VS, FOAMING OVEN TEMP

FIGURE III-7 CELL SIZE VS. FOAMING OVEN TEMP

FIGURE III-8 STRENGTH VS. FOAMING OVEN TEMP

FIGURE III-9 CELL SIZE VS. TIME IN FOAMING OVEN

FIGURE III-10 STRENGTH/DENSITY VS. TIME IN FOAMING OVEN

FIGURE III-11 DENSITY VS. TIME IN FOAMING OVEN

IV. THERMODYNAMICS OF FOAM FORMATION

Introduction

The formation of a foam cell occurs in two stages: nucleation and growth. During the nucleation stage, the bubble embryo grows from a region of high gas concentration to a stable cell having distinct boundaries. The cell then grows by diffusion of the gas from the surrounding supersaturated matrix, and finally by relaxation of the matrix.

To enable a cell to form, the decrease of supersaturation must supply the energy needed to form the cell and effect the accompanying entropy rise. Obeying the second law of thermodynamics, the entropy of an isolated system at constant temperature must increase above $\int_1^2 dQ/T$ during an irreversible process. The excess energy contributed to entropy is a criterion for determining the spontaneity of the process; the greater the energy excess, the more readily the reaction can take place. Classical nucleation theory is based on this concept. Under highly irreversible conditions, when large amounts of excess energy are usurped by entropy, bubbles form quite rapidly. If the process is reversible, bubbles will be nucleated at a rate of zero (i.e., they will collapse as quickly as they are formed). If not enough energy is available to produce the necessary entropy rise, bubbles will not form unless energy is added to the system.

A. Determination of Gibb's Free Energy

The amount of excess energy contributed to entropy can be calculated by combining first and second laws of thermodynamics.

$$T\Delta\underline{S} - \Delta\underline{E} - \Delta W = \text{excess entropic energy} \geq 0 \qquad \text{(IV-1)}$$

For a system at constant temperature and pressure, and for which there is no shaft work (so $\Delta W = P\Delta V$, pressure times the change in volume), the excess entropic energy just described is the negative of the change in Gibb's free energy (G).

$$\Delta\underline{E} + P\Delta V - T\Delta\underline{S} = \Delta G)_{T_o, P_o} \qquad \text{(IV-2)}$$

G is defined by

$$G \equiv U + PV - T\underline{S} \qquad \text{(IV-3)}$$

Thus, for a reaction to occur without additional energy input, ΔG must be negative. For it to occur rapidly, ΔG must be large and negative.

The conditions on which ΔG depends are the concentration of the gas (X), the solubility of the gas in the matrix (K), the surface energy coefficient (γ), the dynamic modulus (E) of the matrix material, temperature (T) and the radius of the bubble (R) after nucleation is complete. Dimensional analysis yields units of energy from the following combinations of those parameters:

$$X \cdot T \cdot RR^3$$
$$KTR\gamma R^2$$
$$KTRER^3$$
$$\gamma R^2$$
$$ER^3$$

Where R is the universal gas coefficient. Thus, for large bubble radii, contributions from concentration, solubility and dynamic modulus are expected to dominate the expression for ΔG. For small bubble radii, the surface energy coefficient and solubility will be more important.

ΔG will be calculated to understand the contributions of each of these factors more explicitly. The system to be used for this calculation is a volume of solution (V_0) and the gas it contains. The system is assumed both adiabatic and isolated from gas transfer. The volume, V_0, is such that it supplies all of the gas that bubble needs, but is not larger than necessary to do this. It is assumed that the system will change quasistatically from an unfoamed state (state 1) to a state containing one gas bubble with distinct surface boundaries (state 2). The following assumptions will also be made:

In state 1:

A) The solution is uniform and ideal (i.e., it follows Henry's law).

B) The temperature and pressure are uniform throughout the system.

In state 2:

A) Even though gas has left the solution matrix, the matrix is incompressible, so the volume of state 2 is V_0 plus V_b, where V_b is the volume of the bubble.

B) The gas contained in the bubble is ideal. The matrix surrounding the bubble is still a uniform, ideal solution (albeit with a lower concentration of gas).

C) The system is adiabatic and temperature change is negligible

(temperature is therefore still uniform).

D) Pressure is uniform in the solution surrounding the bubble.

One final assumption bears some discussion. It was assumed that the nucelation process takes place so rapidly that no gas diffuses to the nucleation site. Such an assumption means that nucleation consists only of forcing the matrix material from the region which will ultimately be the bubble, leaving behind the gas which will fill the bubble. Thus, the volume of polymer forced from the bubble region had to contain enough gas to fill the bubble (plus any residual gas which was ushered out with the polymer). This means that the initial volume of the system, chosen to be only that plastic which supplies gas to the bubble, is that of the final bubble size. The final volume, V_2, of the system is therefore twice that of the bubble size, or $8/3 \pi R^3$. Note that the assumption that no diffusion takes place means that no concentration gradient develops in the exiting plastic.

The minimum concentration necessary for bubble nucleation is

$$X_m = \frac{Nb}{V_b} + X_R \qquad \text{(IV-4)}$$

Where N_b is the number of moles of gas molecules in the bubble, and X_R is the residual gas concentration. Since the gas was assumed ideal,

$$N_b = \frac{P_b \cdot V_b}{RT} \qquad \text{(IV-5)}$$

By Henry's law, $X_R = P_b K$, where K is a constant determined in Appendix E.

$$X_m = \frac{P_b}{RT} + P_b K = P_b \left(\frac{1}{RT} + K\right) \qquad \text{(IV-6)}$$

Henry's law has been experimentally shown to be a good approximation for the polymer-gas systems considered in this work (Frisch, 1965).

The change in Gibb's free energy for the process is the difference between the free energy of the final and initial states. Calculating the Gibb's free energy for the first state is fairly straightforward. The energy stored in the system, $\underline{E}$, is simply the internal energy, U. For an ideal solution of two components,

$$\underline{E}_1 = U_1 = \sum_{i=1}^{2} \mu_i n_i - PV + T\underline{S} \qquad \text{(IV-7)}$$

where μ_i is the chemical potential of the ith component and n_i is the number of molecules of that component (Denbigh, 1968; Hatsopoulos and Keenan, 1965). Since the PV and TS terms cancel when this is substituted into the definition of Gibb's free energy,

$$G_1 = \sum_{i=1}^{2} \mu_i n_i \qquad \text{(IV-8)}$$

For the second state, the Gibb's free energy is most easily calculated by realizing that it is the sum of two parts, the free energy of the solution (including the surface of the bubble), G_s, and the free energy of the gas, G_g.

The energy, $\underline{E}_s$, stored in the solution is the internal energy of the solution plus the energy stored in the elastic deformation (D) plus the surface energy (S). So

$$\underline{E}_s = \sum_{i=1}^{2} \mu_1 n_1 - PV + T\underline{S} + D + S \qquad (IV-9)$$

Thus, the Gibb's free energy accommodated in the solution is

$$G_s = \sum_{i=1}^{2} \mu_{i_2} n_{i_2} + D + S \qquad (IV-10)$$

Where the subscript 2 denotes state 2.

The energy contained in the gas in the bubble is the same as that of a mixture with one component.

$$\underline{E} = \mu_g n_b - PV + T\underline{S} \qquad (IV-11)$$

where n_b is the number of gas molecules in the bubble, and μ_g is the chemical potential of the gas. For an ideal gas, the chemical potential is the potential at a reference pressure (μ_0) plus the potential arising from the difference between the actual pressure and the reference pressure (RTlnp),

$$\mu_g = \mu^0 + RTlnp \qquad (IV-12)$$

Thus, combining equations 11 and 12, the Gibb's free energy for the gas in the bubble is,

$$G_g = \mu^0 n_b + n_b RTlnp_b$$

The total Gibb's free energy for the system at the second state is therefore,

$$G_2 = G_s + G_g = \mu^0 n_b + \sum_{i=1}^{2} \mu_{i_2} n_{i_2} + D + S + n_b RT\ln p_b$$

$$(IV-13)$$

The change in G for the process is the difference between G_1 and G_2:

$$\Delta G = G_2 - G_1 = \mu^0 n_b + n_b RT\ln p_b + \sum_{i=1}^{2} \mu_{i_2} n_{i_2} + D + S$$

$$- \sum_{i=1}^{2} \mu_{i_1} n_{i_1} \qquad (IV-14)$$

Since the solutions follow Henry's law, it is possible to substitute more meaningful expressions for the chemical potential, namely, express μ in terms of concentration.

First, the summation terms can be simplified by making the assumption that the gas concentration is low. Thus, as the gas leaves, the concentration of polystyrene does not change significantly. Since the number of polystyrene molecules remains constant, $n_{ps}\mu_{ps}$ is the same for state one and state two. Those terms cancel, leaving

$$\Delta G = \mu^0 n_b + \mu_{g_2} n_{g_2} + D + S - \mu_{g_1} n_{g_1} + n_b RT\ln p_b \qquad (IV-15)$$

For any component of an ideal solution, the chemical potential is the potential of that component alone plus the potential gained due to mixing.

$$\mu = \mu^* + RT\ln X$$

where X is the concentration of the gas, and μ^* is the chemical potential of the pure component. So,

$$\Delta G = \mu^0 n_b + n_b RT\ln p_b + n_{g_2}(\mu^* + RT\ln X_2) - n_{g_1}\mu^* + RT\ln X_1 + D + S$$

$$(IV-16)$$

This can be made simpler still. Since the solution is ideal, there is no interaction between the gas and the plastic. The gas will behave as though it were in a mixture of ideal gases, and its chemical potential can be expressed as that of one component of an ideal gas mixture.

$$\mu = \mu^0 + RT\ln p_i$$

(where p_i is the partial pressure of the gas). Therefore, ΔG can also be expressed as

$$\Delta G = \mu^0 n_b + n_b RT\ln p_b + n_{g_2}(\mu^0 + RT\ln p_b) - n_{g_1}(\mu^0 + RT\ln p_1)$$

$$+ D + S \qquad\qquad (IV-17)$$

---

1. Note that $RT\ln X$ is negative since $X < 1$, so the chemical potential actually decreases when substances are mixed. This is because entropy must increase.

where p_1 is the partial pressure of the gas at state 1.

Since $n_{g_1} = n_{g_2} + n_b$,

$$\Delta G = n_{g_1} RT(\ln p_b - \ln p_1) + D + S$$

$$= n_{g_1} RT \ln(p_b/p_1) + D + S \qquad\qquad (IV-18)$$

Henry's law equates p with KX, so

$$\Delta G = n_{g_1} \cdot RT \ln(X_2/X_1) + D + S \qquad\qquad (IV-19)$$

Only those conditions which force this expression to be negative will allow nucleation to occur. Many of the quantities in the above expression depend upon the final radius of the nucleated cell. Are there certain radii which will not be nucleated?

In order to answer this question, it is necessary to express the dependent variables in terms of R. All of the quantities except T, K, R, and X, depend upon R. T is assumed in variant. K is a material property R is the universal gas constant, and X_1 is an initial condition.

The dependency of n_b, n_{g_2}, n_g, and X_2 can be determined using three conditions:

1. The number of gas molecules in the system remains fixed.

2. Henry's law applies to the system.

3. The work done by the bubble to the surrounding solution is $\int p_b dV$.

From condition 1, the number of gas molecules in bubble, n_b is the difference between the number of molecules residing in the final and initial solutions, n_{g_2} and n_{g_1}. These quantities, n_{g_2} and n_{g_1} are related to the concentrations, X_1 and X_2 by,

$$X_1 = n_{g_1}/V_o \tag{IV-20a}$$

$$X_2 = n_{g_2}/V_o \tag{IV-20b}$$

where V_o is the volume of the polymer solution which supplies gas to the bubble (an assumption is made that the concentration is uniform throughout this volume). Since the solution was assumed ideal,

$$X_2 = p_b/K \tag{IV-21}$$

where p_o is the pressure inside the bubble. Thus, expressions for n_b, n_{g_2}, n_{g_1}, and X_2 in terms of R are as follows:

$$X_2 = p_b/K \tag{IV-22a}$$

$$n_{g_1} = V_o \cdot X_1 \tag{IV-22b}$$

$$n_{g_2} = V_o \cdot p_b/K \tag{IV-22c}$$

$$n_b = V_o(p_b/K - X_1) \tag{IV-22d}$$

To calculate p_b, consider the work done by the gas in moving the boundary of the bubble. This work, $\int p_b dV$, goes into deformation plus surface energy:

$$\int_0^{V_b} p_b dV = D + S \qquad (IV-23)$$

Where V_b is the volume of the bubble. $\int p_b dV$ can be expressed in terms of R since $V = \frac{4}{3} \pi R^3$.

$$\int_0^{R_1} p_b \cdot 4\pi R^2 dR = D + S \qquad (IV-24)$$

Now, differentiating with respect to R_1, and realizing that $S = 4\pi R^2 \gamma$, $\frac{dS}{dR} = 8\pi R\gamma$

$$p_b = \frac{1}{4\pi R^2} \frac{dD}{dR} + \frac{2\gamma}{R} \qquad (IV-25)$$

To calculate the change of the energy of deformation with R, $\frac{dD}{dR}$, use the standard formula,

$$dD = \int_V \sum_{j=1}^{3} \sum_{i=1}^{3} \sigma_{ij} d\varepsilon_{ij} dV \qquad (IV-26)$$

Continuity and the assumed incompressibility of the plastic will be used to determine strain as a function of R. The plastic will be modeled as a Maxwell solid to determine stresses from the expressions for strain. These expressions will be substituted into the above formula so it can be evaluated.

The plastic is above T_{g_1} so it should be modeled as a visco-elastic plastic solid. The mechanical analog of one example of such a solid is depicted

friction element

However, for simplicity, the material will be modeled as a Maxwell solid,

In this model, at the instant of loading, the energy is stored elastically, then is dissipated through viscous deformation. Thus, the work done can be approximated by just considering the elastic part of the model (the spring). Although the pressure within the bubble will decrease as the strained plastic surrounding the bubble relaxes, the approximation will be reasonable if the inflation takes place rapidly. So, the stresses will be approximated by those of an elastic solid using a dynamic modulus, E, which is assumed to depend only upon temperature. So,

$$\varepsilon_{11} = \frac{\sigma_{11}}{E} \text{ , etc.} \qquad (IV-27)$$

The generalized expressions for strain in spherical coordinates are

$$\varepsilon_{rr} = \frac{\partial u_r}{\partial r}, \varepsilon_{\phi\phi} = \frac{1}{r}\frac{\partial u_\phi}{\partial_\phi} + \frac{u_r}{r} \tag{IV-28a}$$

$$\varepsilon_{\theta\theta} = \frac{1}{r_{\sin\theta}}\frac{\partial u_\theta}{\partial_\theta} + \frac{u_r}{r} + \frac{u_\theta}{r}\cot\phi \tag{IV-28b}$$

$$\varepsilon_{r\theta} = \frac{1}{2}\left[\frac{1}{r_{\sin\phi}}\frac{\partial u_r}{\partial\theta} + \frac{\partial u_\theta}{\partial r} - \frac{u_\theta}{r}\right] \tag{IV-28c}$$

$$\varepsilon_{r\phi} = \frac{1}{2}\left[\frac{\partial u_\phi}{\partial r} - \frac{u_\phi}{r} + \frac{1}{r}\frac{\partial u_r}{\partial\phi}\right] \tag{IV-28d}$$

$$\varepsilon_{\phi\theta} = \frac{1}{2}\left[\frac{1}{r}\frac{\partial u_\theta}{\partial\phi} - \frac{u_\theta}{r}\cos\phi + \frac{1}{r_{\sin\phi}}\frac{\partial u_\phi}{\partial\theta}\right] \tag{IV-28e}$$

As the bubble expands, however, the only movement is in the radial direction, so $u_\phi = u_\theta = 0$, and the above expressions reduce to

$$\varepsilon_{rr} = \frac{\partial u_r}{\partial r}, \; \varepsilon_{\phi\phi} = \frac{u_r}{r} = \varepsilon_{\theta\theta} \tag{IV-29a, b}$$

$$\varepsilon_{r\theta} = \varepsilon_{r\phi} = \varepsilon_{\phi\theta} = 0 \tag{IV-29c}$$

Substituting these expressions back into that for dD,

$$dD = \int_V \frac{\partial u_r}{\partial r} Ed\varepsilon_{rr}dV + \int_V \frac{u_r}{r} Ed\varepsilon_{\theta\theta}dV + \int_V \frac{u_r}{r} Ed\varepsilon_{\phi\phi}dV \tag{IV-30}$$

The strains can be evaluated in terms of R by invoking continuity and the assumption that the plastic is incompressible. The volume of plastic which was contained in the bubble must move outward. That volume must cross a control sphere drawn at any radius, r. From the geometry

shown in Figure IV-1 , the volume can be expressed as

$$V_b = \int_r^{r + u_r} 4\pi r^2 dr \qquad \text{(IV-31a)}$$

or

$$\frac{4}{3}\pi R^3 = \frac{4}{3}\pi[(r + u_r)^3 - r^3] \qquad \text{(IV-31b)}$$

(Note that R is the final bubble radius whereas r is the radial coordinant, a variable.) The resulting equation,

$$0 = 3u_r r^2 + 3u_r^2 r + (u_r^3 - R^3)$$

can be solved for u_r by using the cubic formula. After the ensuing algebra, and discarding the imaginary terms,

$$u_r = (r^3 + R^3)^{1/3} - r$$

From this result, the strains are

$$\varepsilon_{rr} = \left(1 + \frac{R^3}{r^3}\right)^{-2/3} - 1 \qquad \text{(IV-32a)}$$

$$\varepsilon_{\theta\theta} = \varepsilon_{\phi\phi} = \left(1 + \frac{R^3}{r^3}\right)^{1/3} - 1 \qquad \text{(IV-32b)}$$

$$d\varepsilon_{rr} = -2\left(1 + \frac{R^3}{r^3}\right)^3 \frac{R^2}{r^3} dR \qquad \text{(IV-32c)}$$

FIGURE IV-1 GEOMETRY FOR CALCULATING STRAIN IMPOSED
BY SPHERICAL GROWTH

$$d\epsilon_{\phi\phi} = d\epsilon_{\theta\theta} = \left(1 - \frac{R^3}{r^3}\right)^{-2/3} \frac{R^2}{r^3} \, dr \qquad \text{(IV-32d)}$$

These can be substituted into the expression for dD.

$$dD = \int_V \left| \left| \left(1 + \frac{R^3}{r^3}\right)^{-2/3} - 1 \right| E \left| -2 \left(1 + \frac{R^3}{r^3}\right)^{-5/3} \frac{R^2}{r^3} \right| \right| dR \qquad \text{(IV-33)}$$

$$+ 2 \int_V \left| \left| \left(1 + \frac{R^3}{r^3}\right)^{1/3} - 1 \right| E \left| \left(1 - \frac{R^3}{r^3}\right)^{-2/3} \frac{R^2}{r^3} \right| \right| dR$$

Integrating by numerical methods (the program is shown in Appendix F),

$$dD \doteq 12R^2 E dr \qquad \text{(IV-34)}$$

The pressure inside the bubble can therefore be evaluated as

$$P_b = \frac{12ER^2}{4\pi R^2} + \frac{2\gamma}{R} = \frac{3E}{\pi} + \frac{2\gamma}{R} \qquad \text{(IV-35)}$$

Substituting this to obtain X_2, n_{g_2}, and n_b,

$$X_2 = \frac{3E}{\pi K} + \frac{2\gamma}{RK} \qquad\qquad \text{(IV-36a)}$$

$$n_{g_2} = V_0 \left(\frac{3E}{\pi K} + \frac{2\gamma}{RK} \right) \qquad\qquad \text{(IV-36b)}$$

$$n_b = V_0 \left(\frac{3E}{\pi K} + \frac{2\gamma}{RK} - X_1 \right) \qquad\qquad \text{(IV-36c)}$$

Recall that V_0 was defined as the volume of the polymer solution which supplies gas to the bubble. Since it was assumed that no gas diffuses to the bubble embryo during nucleation, this volume is $\frac{4}{3} \pi R^3$. So,

$$n_{g_1} = \frac{4}{3} \pi R^3 X_1 \qquad\qquad \text{(IV-37a)}$$

$$n_{g_2} = 4 \, ER^3/K + \frac{8\pi}{3K} \gamma R^2 \qquad\qquad \text{(IV-37b)}$$

$$n_b = 4 \, ER^3/K + \frac{8\pi}{3K} \gamma R^2 - \frac{4}{3} \pi R^3 X_1 \qquad\qquad \text{(IV-37c)}$$

The two other quantities which depend on R, the surface energy, S, and the deformational energy, D, have been evaluated during the course of this discussion.

$$S = 4\pi R^2 \gamma \qquad\qquad\qquad\qquad (IV\text{-}38)$$

$$D = \int \frac{dD}{dR}\, dR = 4\, E R^3 \qquad\qquad\qquad (IV\text{-}39)$$

All of these values can now be substituted into the expression for ΔG to obtain an expression which depends on R.

$$\Delta G = \frac{4}{3}\pi R^3 X_1 \quad RT \ln\left[\frac{\frac{3E}{\pi} + \frac{2\gamma}{R}}{KX_1}\right] + \frac{4}{3}E R^3 + 4\pi R^2 \gamma \qquad (IV\text{-}40)$$

The values, X, K, γ and E, which do not depend on R are all controlled by the foaming conditions. To determine under what conditions foam can be produced, ΔG was evaluated for incremental values of R and various values of X_1, K_1 γ and E. The calculation was made in APL on the MULTICS systems at MIT. (The program is called PROG and is in Appendix D.)

Typical ΔG versus R curves are shown in Figure IV-3. For 2 moles/cm^3 ΔG becomes negative at 1.45×10^{-4} μ (5.7×10^{-9} in). In order to satisfy the energy balance without obtaining energy from external sources, the cells must nucleate to this raduis. However, ΔG goes through a metastable equilibrium point at 1.05×10^{-4} μ (4.13×10^{-9} in). If a cluster of gas molecules should occur with a raduis greater than this, say $1.1 \times 10^{-4} \mu$ (even if it had to gain energy from the environment to reach this configuration), they will be stable and continue to grow.

FIGURE IV-2   CHANGE IN GIBB'S FREE ENERGY VS. RADIUS
OF BUBBLE EMBRYO

Thus, 2.16×10^{-3} μ is the minimum cell size attainable from these conditions; all smaller embryos will decrease in size until they are completely reabsorbed.

What happens if the conditions change? In Figure IV-3, the ΔG versus R curves have been plotted for increasing gas concentrations. Since the energy content of the gas per mole increases as the concentration increases, the amount of gas needed to overcome the surface tension decreases. Consequently, the critical radius decreases with increasing concentration. This is plotted in Figure IV-4. Since the energy released by the gas is a volumetric quantity, roughly proportional to R^3 (this is only approximate since the final concentration is a function of R), and the surface energy is proportional to R^2, the curve is a hyperbola. This is shown more clearly on the log-log plot in Figure IV-5.

Also involved in the energy balance (and hence the expression for ΔG) is the deformational energy. This is also a volumetric term, as shown by the dimensional analysis discussed earlier. This term subtracts from the energy gained by reducing the gas concentration, and the resulting quantity must overcome the increase in surface energy. If CR^3, DR^3 and SR^2 are the energies associated with concentration charge, deformation, and surface formation, respectively, then

$$(C - D)R^3 - SR^2 \geq 0 \qquad\qquad (IV-41)$$

In the plot of critical radius versus concentration, only C was allowed

FIGURE IV-3   CHANGE IN GIBB'S FREE ENERGY VS. BUBBLE EMBRYO RADIUS
FOR VARYING GAS CONCENTRATIONS

FIGURE IV-4 CRITICAL RADIUS VS. CONCENTRATION

to change. If C is held constant, instead, and D is increased, then the energy gained per mole of gas evolved decreases. Thus, the critical radius must grow larger and larger until finally, D equals C, and foam can no longer be produced. A plot of this is in Figure IV-6. This is why cells do not form until the supersaturated plastic is heated.

B.   Production of Cell Size Distributions

During the preceeding discussion, it was shown that nucleated cells must be larger than some minimum size. This size was determined for various conditions. Of more interest however, is the size to which these cells grow after they have been nucleated and the distribution the sizes will follow.

Bubbles may be nucleated so long as the appropriate conditions prevail. If the conditions prevail for five minutes, then the bubbles formed initially will have five minutes more diffusion than those formed at the end of the time. To determine the cell size distribution, therefore, it is necessary to determine the rate of nucleation and how much gas diffuses to the cells per unit time (their growth rate).

a)   The Rate of Nucleation

In order to determine the nucleation rate, one must rely on statistical mechanics. Homogeneous nucleation theory was first established for condensation of droplets from the vapor phase, and then extended to other systems. The original theory was developed by Volmer (1939), Farkas (1922), Becker and Doring (1935) and Zeldovich (1943). They based their work on Gibb's realization that the spontaneity of a

process is proportional to exp (-ΔG/kT). Excellent reviews of the development of nucleation theory have been made by Zettlemoyer (1969), Blander and Katz (1975), Cole (1974), Reid (1978), and Russell (1980).

The crucial question in determining the rate of nucleation is "how often does a cluster of gas molecules grow large enough to exceed the critical radius?" Following the derivation of Zeldovich (1949) to determine this, one must look at the rate nucleii grow as a function of size. The net rate at which bubble embryos one molecule smaller than the critical size gain that last molecule is the nucleation rate. The embryo growth rate can be expressed as the difference between the rate molecules join the cluster and the rate they leave. If the joining rate per unit surface is β, and the leaving rate $\underline{\gamma}$, f is the distribution of nuclei sizes, and η is the size of a critical cell, the rate of cell nucleation, J, equals

$$J = f(\eta-1) \; \beta(\eta-1) \; S(\eta-1) - f(\eta) \; \underline{\gamma}(\eta) \; S(\eta) \tag{IV-42}$$

where $S(\eta)$ is the surface area of a cell of size η.

For a dilute substance dissolved in a liquid, Reiss (1950) has shown that

$$\beta = \frac{3}{2} \frac{D}{|\ell|} X$$

where D is the diffusion rate and $|\ell|$ is the mean jump length, and can be approximated by the distance between equilibrium positions in the

liquid lattice. In the case of a polymer, this would be the mean distance between adjacent molecules (see Figure IV-7). Assuming that the styrene units are uniformly distributed throughout the volume, each polystyrene unit has 1.23×10^{-22} ml associated with it. If they are uniformly packed, each unit is in the center of a sphere, and the distance between units is 6.9×10^{-8} cm. This will be slightly lower than the distance between polymer chains since the units will be packed more tightly along the molecular axis. However, the bulkiness of the unit was not taken into consideration. Neither β_c S_c, N_0 nor Z need to be known with great accuracy since the exponential factor will dominate the equation. β_c is therefore approximately

$$\beta_c = \frac{3}{2} \frac{\mathcal{D}}{6.91 \times 10^{-8} \text{ cm}} \cdot X \qquad \text{(IV-43)}$$

$\mathcal{D}$ is the diffusion coefficient and is discussed in Appendix F. X is the concentration of the gas in the polymer and is a variable.

The rate at which gas molecules leave the embryo can be determined for equilibrium conditions when the nucleus does not grow. It is assumed that this rate remains the same independent of whether an equilibrium number of bubbles exists or not. Still following the derivation of Zeldovich (1949), at equilibrium,

$$J = 0 = N(\eta-1) \, \beta(\eta-1) \, S(\eta-1) - N(\eta) \, \gamma(\eta) \, S(\eta) \qquad \text{(IV-44)}$$

where $N(\eta)$ is the equilibrium number of nucleii of size η. Thus,

$$\underline{Y}(n) \quad = \quad \frac{N(n-1)\ S(n-1)\ \beta(n-1)}{N(n)\ S(n)} \qquad\qquad (IV\text{-}45)$$

Using this value for non-equilibrium situations,

$$J \quad = \quad F(n-1)\ \beta(n-1)\ S(n-1)\ -\ f(n)\ \frac{N(n-1)\ S(n-1)\ \beta(n-1)}{N(n)\ S(n)}\ S(n) \quad (IV\text{-}45a)$$

$$= \quad N(n-1)\ \beta(n-1)\ S(n-1)\ \left| \frac{f(n-1)}{N(n-1)} - \frac{f(n)}{N(n)} \right| \qquad (IV\text{-}46b)$$

If r >> 1, this may be regarded as a derivitive.

$$J \quad = \quad -N_c \beta_c S_c \ \left| \frac{d}{dn} \left(\frac{f}{N} \right) \right|_c \qquad\qquad (IV\text{-}47)$$

where the subscript c indicates that the quantity be that at the critical radius.

As equilibrium, the number of nuclii of critical size is given by

$$N(n) \quad = \quad N_o\ \exp\left[\frac{-\Delta G(n)}{KT} \right] \qquad\qquad (IV\text{-}48)$$

where N_o is the number density of the available nucleation sites in the liquid.

Writing in a more explicit form, one obtains a differential equation

$$J \quad = \quad -N_o\ \exp\left[\frac{-\Delta G(n)}{KT} \right] \cdot \frac{3}{2}\ \frac{D}{|\ell|}\ X \cdot S_c\ \left| \frac{d}{dn} \left(\frac{f}{N_o\ \exp \frac{-\iota\ ?}{KT}} \right) \right|_c \qquad (IV\text{-}49)$$

N_0, K, T, D and $|\ell|$ are all constants. ΔG, and S_c depend upon X, and were calculated already during the determination of the critical radius.

Equation 47 can be solved by integration over all embryo sizes from 0 to infinity. At very small sizes, f is very close to equilibrium, so f/N = 1. At large sizes, f is small compared to N, so f/N = 0. The integration of Equation IV-47 is therefore

$$\int_0^\infty \frac{d\eta}{N\beta S} = -\int_1^0 \frac{1}{J} d\left(\frac{f}{N}\right) = \frac{1}{J} \qquad \text{(IV-50)},$$
$$\text{(IV-51)}$$

Assuming that the rate of nucleation is independent from the similarity of the actual cell distribution to the equilibrium distribution, $\int_0^\infty \frac{d\eta}{N\beta S}$ can be solved numerically. More insight will be gained, however, by approximation using a Taylor's expansion for ΔG. Since the integrand, $1/\beta S N_0 \exp\left[\frac{-\Delta G}{KT}\right]$, has a narrow peak centered around η_c (i.e., around R), an expansion about η_c is satisfactory.

$$\Delta G \doteq \Delta G_c + \left(\frac{\partial^2 \Delta G}{\partial \eta^2}\right)_c \frac{(\eta - \eta_c)^2}{2} \qquad \text{(IV-52)}$$

(The $\left(\frac{\partial \Delta G}{\partial \eta}\right)_c$ term is zero since ΔG is maximum at the critical point). Likewise, β and S can be approximated by their critical values. Moving what is constant in front of the integral sign,

$$\frac{1}{J} = \frac{\exp\left(-\frac{\Delta G_c}{KT}\right)}{\beta_c S_c N_0} \int_0^\infty \exp\left|\left(\frac{\partial^2 \Delta G_c}{\partial \eta^2}\right) \frac{(\eta - \eta_c)^2}{2KT}\right| d\eta . \qquad \text{(IV-53)}$$

Because ΔG is a maximum at the critical point, $\left[\dfrac{\partial^2 \Delta G}{\partial \eta^2}\right]_c$ is negative. The integral therefore involves a gamma function:

$$\int_0^\infty e^{-a^2 t^2}\, dt \;=\; \frac{1}{2a}\,\Gamma\left(\tfrac{1}{2}\right) \;=\; \frac{1}{2a}\,\sqrt{\pi} \qquad\qquad \text{(IV-54)}$$

where

$$a \;=\; \sqrt{-\left[\frac{\partial^2 \Delta G}{\partial \eta^2}\right]_c \cdot \frac{1}{2kT}}$$

and $t = \eta - \eta_c$.

So the nucleation rate is

$$J \;=\; 2\beta_c S_c N_0 \exp\left[\frac{\Delta G_c}{kT}\right] \sqrt{-\left[\frac{\partial^2 G}{\partial \eta^2}\right]_c \Big/ 2kT\pi} \qquad . \qquad \text{(IV-55)}$$

As stated before, β is the rate gas molecules strike the bubble surface.

$$\beta \;=\; \frac{3}{2}\,\frac{D}{|\ell|}\, X \;=\; \frac{3}{2}\,\frac{D}{6.91 \times 10^{-8}\ \text{cm}}\, X \qquad\qquad \text{(IV-56)}$$

S_c is the surface area of a critical bubble, or $3/4\, \pi\, R_c^3$ N_0 is the

density of locations (potential sites for bubble nucleation). A potential

site is any free volume (i.e., volume unoccupied by polymer) in the

matrix which is large enough to contain a gas molecule. The number of

such sites can be estimated by assuming that their size follows a

Gaussian distribution, and that the sum of the volume of all such sites

equals the total free volume of the material (this assumes that the

total volume of sites smaller than one gas molecule is negligible).

Using nitrogen in polystyrene as a typical example, the volume of one

N_2 molecule is 6.59×10^{-24} ml and the volume of one mer of poly-

styrene, 1.32×10^{-23} ml. Since the density of polystyrene is about

one gm/ml, the total number of sites, N_o, is approximately 7×10^{21} sites/

cm^3. This compares favorably with the value of 4×10^{21} cavities/ml

for hydrogen in polyethylene found by Frisch (1965).

Unfortunately, when the program is run with the values typical of

those which produce foam in the laboratory, the rate of nucleation pre-

dicted is negligible. For nucleation to be appreciable, the change

in Gibb's free energy between the initial state and the state with a

cell of critical radius must not be greater than about 60 kT. This was

shown by the program results and mentioned by Russell (1980). In the

laboratory, polystyrene was foamed at 117°C (390°K) after having been

exposed to 2.4×10^7 dynes/cm^2 (350 psi) N_2 gas for 24 hrs. The con-

centration of gas in the polystyrene is not greater than 0.0306 moles/cm^3

(0.00187 moles/in^3) which is the saturation concentration at 2.4×10^7

dynes/cm^2. The dynamic modulus of the material at 393°C is 158 psi

(Waldman, 1980) (Tested on the same run of extruded material as was

used for the experiments reported in this work). According to experimental and theoretical work by Wu (1970), the surface energy coefficient for polystyrene is 33 dynes/cm (1.9×10^{-4} lb/in). However, looking at the program results, nucleation is predicted insignificant for concentrations equal to or less than 4.3×10^{-5} moles/cm^3, even with a modulus of 0 and surface tension as low as 7 dynes/cm (one-fifth of that of polystyrene). The presence of rubber particles lowers the surface energy. Rubber, itself, has a surface tension of 25 dynes/cm (calculated by the parachor method in Appendix A), so the interfacial tension is 8 dynes/cm. The energy stored in this interface contributes to the formation of cells forming there. In the extreme, if the cell could form its surface entirely from interfacial surface, the value for surface tension which should be used in the calculation is 17 dynes/cm (8.46×10^{-5} lb/in) which is still more than twice as high as the value predicted acceptable.

Since the prediction is so far in error, it suggests a flaw in the theory. It may be that the classical nucleation theory does not apply to this case. Larger radii are associated with slower nucleation rates, but even for rates so slow that nucleation is not appreciable (the change of Gibb's free energy > 60 kT), the critical radii are smaller than 25 Å (1×10^{-7} in). A lower bound to the average distance between polymer chains was estimated to be about 7 Å (see page 65). Since the size of the voids in between the polymer molecules follows a random distribution, it is conceivable that voids exist which are the size of the critical radius. The actual distribution of cavities

as a function of size should be determined to see if this argument is plausible. Since this requires extensive study of the conformational statistics of polymer chains, it is beyond the scope of this work. It is also questionable whether the concept of surface energy can still be employed, or whether Gibb's free energy must likewise be calculated from statistical considerations.

b) Growth by Diffusion

Once they are nucleated, cells grow by diffusion from the matrix. It was assumed that each cell is surrounded by a diffusion zone across which no gas flows, that all diffusion zones are the same size, and that they are arranged in a close-packed configuration. The size of the zones is determined only by cell density.

This mode has several limitations which restrict it to short diffusion times. First of all, it does not take into account the fact that larger cells have lower internal pressures and thus higher potential for diffusion (Hobbs, 1975). Also, it does not account for the movement of gas not in a diffusion zone, and it makes the assumption that the cells are regularly spaced.

The concentration distribution is found by applying the diffusion equation to the diffusion zone. Since the region was spherical and uniform, advantage can be taken of the symettry to drop the angular terms, leaving

$$\frac{\partial x}{\partial t} = D\ \frac{\partial^2 x}{\partial r^2} + \frac{2}{r}\frac{\partial x}{\partial r} \qquad\qquad (IV\text{-}57)$$

The boundary conditions for the zone are that the concentration at the edge of the cell is the solubility, K, times the pressure in the cell. The restriction that no gas can cross the outside boundary of the zone imposes the condition that the concentration gradient be zero at that boundary. The initial condition is the concentration gradient shown in Figure IV-9. The concentration has the initial value, C_0, everywhere except in the depleted region, as shown.

This was solved with a series solution (Hildebrandt, 1964). The particular solutions were of the form:

$$X(r_1\varepsilon) = \frac{A_\lambda e^{-\lambda^2 v t}}{\lambda r} \left| -\tan(\lambda R)\cos(\lambda r) + \sin(\lambda r) \right| \qquad \text{(IV-58)}$$

and orthogonal in the region of interest. λ was found from the characteristic equation

$$\tan\lambda R = \frac{\tan(\lambda r_1) - \lambda r_1}{\lambda r_1 \tan(\lambda r_1) + 1} \qquad \text{(IV-59)}$$

The coefficients, A_λ, were found from

$$A_\lambda = \frac{C_0 \int_R^{r_1} r^2 dr k_\lambda(r)}{\int_R^{r_1} r^2 dr R_\lambda(r)^2} \qquad \text{(IV-60)}$$

where
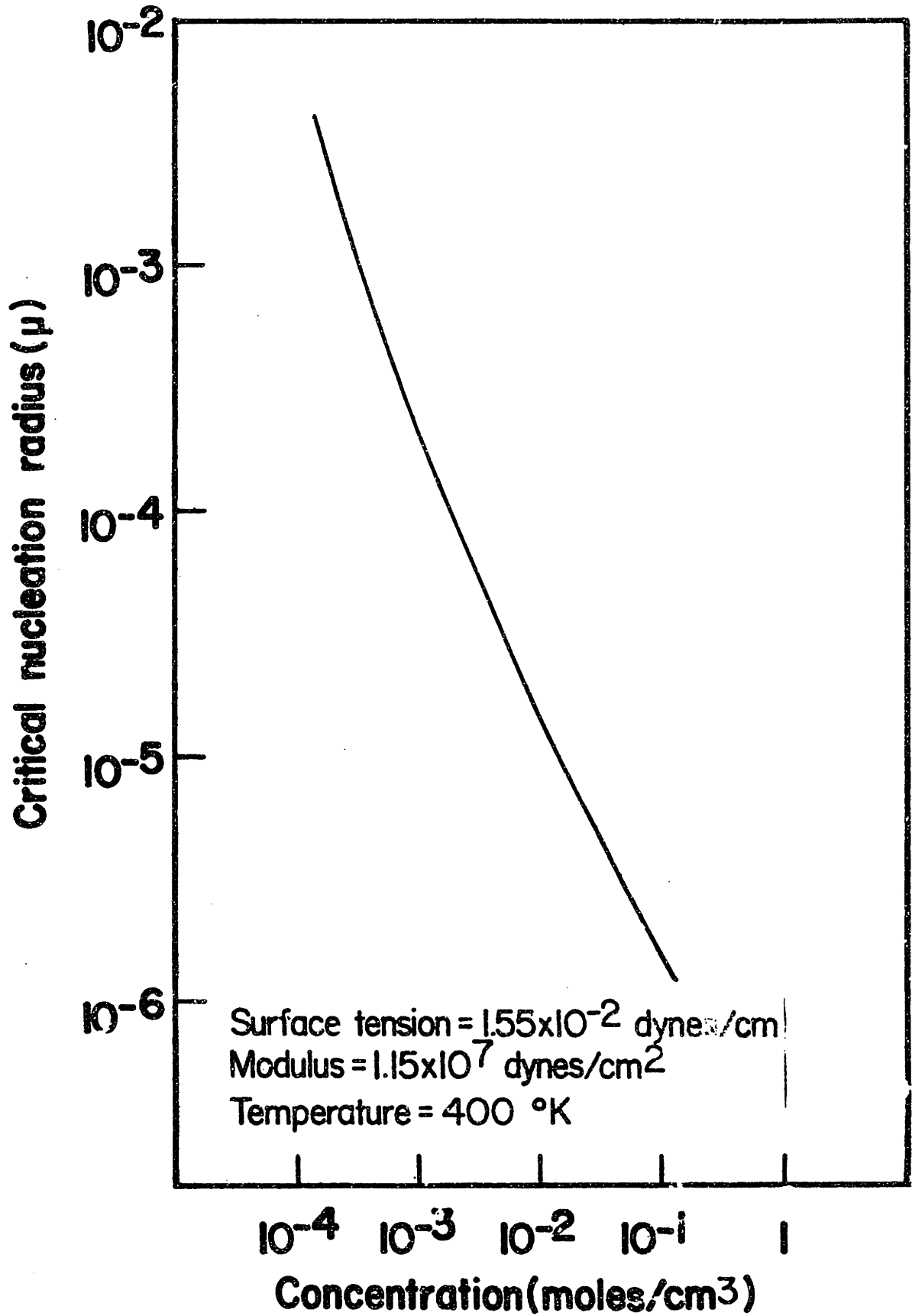
FIGURE IV-5 CRITICAL RADIUS VS. CONCENTRATION (LOG PLOT)
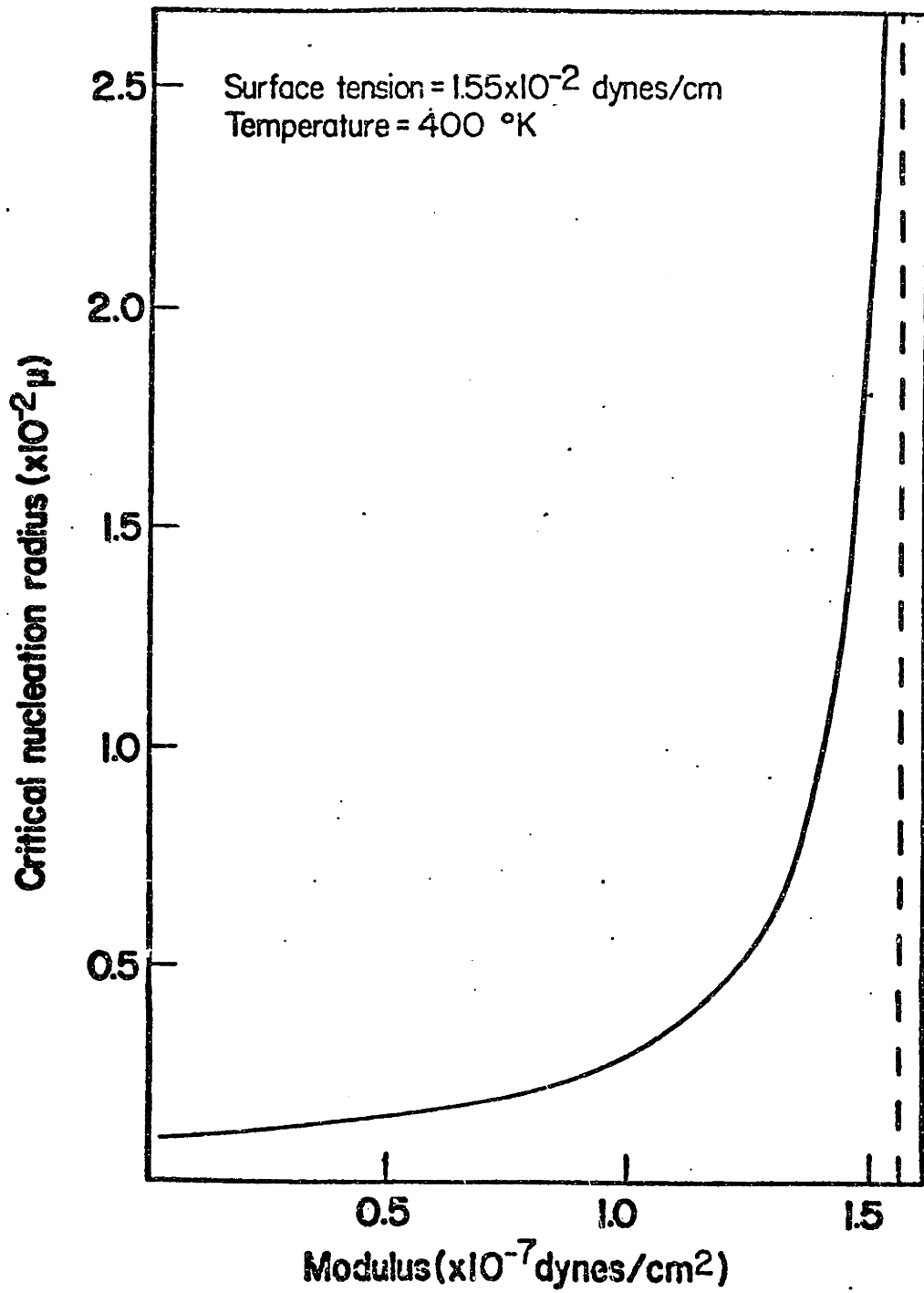
FIGURE IV-6   CRITICAL RADIUS VS. MODULUS

The average of all " ↔ 's" is $|\ell|$, the mean jump length.

FIGURE IV-7 MEAN JUMP LENGTH

FIGURE IV-8   DIAGRAM OF DEPLETED REGIONS AND DIFFUSION ZONES

FIGURE IV-9 CONCENTRATION GRADIENT

FIGURE IV-10 PARTICULAR SOLUTIONS TO DIFFUSION EQUATION WHEN T = 0

$$R_\lambda = \frac{-\tan(\lambda R)\cos\lambda r + \sin\lambda r}{\lambda r} \qquad \text{(IV-61)}$$

For typical values, the first four terms at t = 0 are shown in Figure IV-1C.

c) A Computer Model

A model was developed which combines nucleation rate with diffusional growth to determine the cell size distribution. It was programmed on the MULTICS system at MIT in APL.

For successive time increments, the program calculates the number of cells nucleated and the diffusional growth which occurs during each increment. Since the cells first nucleated will grow largest (and since the amount of diffusion depends on the radius of the cell), the amount of growth is calculated separately for each time increment, the gas concentration is adjusted to account for the nucleation and growth. The program and a detailed discussion of it are found in Appendix C.

The program uses search routines to determine the λ's in the diffusion equation. Unfortunately, after the program was completed in APL, it was found that the number of λ's needed to obtain sufficiently accurate concentration profiles was high (at least 12). Since the search routines are lengthy ($\sim$ 3 hours), obtaining the cell size distribution for one set of conditions would take the better part of a weekend. Neither the time nor the computer funds were available for a complete set of data points calculated this way. Although the work could be reprogrammed in a more efficient language, enough had been learned about the calculation to enable making some additional assumptions and doing part of the calcula-

tion by hand. The assumptions and calculation methods will be desribed, followed by a description of the results.

Before delving into that topic, however, it is important to realize that there are three stages during foam formation and growth: nucleation, diffusional growth, and matrix relaxation. Nucleation is the transformation of small clusters of gas molecules to energetically stable pockets of molecules with distinct cell walls. The second stage is that of diffusional growth. During this period the bulk of the gas moves out of the matrix and into the cells until equilibrium exists between the concentration of gas in the matrix and the internal pressure in the cells. The third stage is growth by relaxation of the matrix. Relaxational growth allows the material around the cells to lose its orientation, whereas nucleation and deformational growth both impose orientation.

The program follows foam formation through the first two periods. It determines the number of cells nucleated, then calculates the amount of gas which diffuses to each cell. It is important to gain an accurate estimate of the total number of cells nucleated to be able to predict their final size.

The program uses classical nucleation theory to predict the cell nucleation rate from concentration and other system parameters (see Section IV.B.a). That theory shows that the ultimate cell density is limited by the gas concentration in the matrix. Only when the concentration exceeds a certain minimum value will nucleation occur. It was assumed that nucleation does occur, even when the concentration exceeds the limit only locally. Nucleated cells deplete the local region of gas and

attract gas by diffusion. Between the cells, the concentration will drop with time. Thus, the ultimate cell density depends heavily on both the Gibb's free energy barrier and the rate of diffusion of the gas through the matrix.

Three regimes of foaming behavior can be established by comparing the nucleation rate with the rate of diffusion. When the nucleation rate is slow (less than 2×10^{12} cells/in^3sec), the few cells which nucleate are widespread, and it takes a long time for diffusion to bring the system into equilibrium. By the time equilibrium is reached, relaxation of the matrix is already significant. Such low nucleation rates produce foams of poor quality with large, widely spaced cells. If the nucleation rate is high, cells will develop so fast that the diffusion length ($\sqrt{Dt}$ where t is the duration of nucleation) is less than the thickness of the depleted region. In this case, nucleation is halted when depleted regions interfere with each other. For intermediate nucleation rates (greater than 2×10^9 and less than 2×10^{16} cells/in^3 sec for the polystyrene - N_2 system studied) diffusion is of the same order as the rate of nucleation. The diffusion process is well underway by the time nucleation stops. In fact, nucleation halts because diffusion significantly lowers the gas concentration in the matrix.

The program is most successful in the middle regime. For high or low rates of nucleation, simplifying assumptions make the computer program inapplicable.

Since the program does not make a detailed analysis of the concen-

tration distribution in the depleted region, its estimate of the final cell density in quickly nucleated foams is dictated by an arbitrary choice of concentration distribution. A simpler and more consistant method for calculating the ultimate cell densities in these foams is to assume that nucleation halts once the depleted regions interfere with one another. This can be calculated easily by hand.

The total number of cells nucleated can be estimated by assuming a close packed configuration of spheres the size of the depleted region. Using the argument as proposed in Appendix B to calculate the distance between closepacked cells,

$$\rho \text{ cell} = \frac{1}{4\sqrt{2}\ r_d^3} \qquad \text{(IV-62)}$$

where here, r_d, is the radius of the depleted region. For one unit volume of completely nucleated foam, the gaseous volume is

$$\rho \text{ cell} \cdot \frac{4}{3}\pi R^3 \qquad \text{(IV-63)}$$

where R is the cell radius. The remaining volume is the matrix, so

$$\rho_m = 1 - \rho \text{ cell} \cdot \frac{4}{3}\pi R^3$$

$$= 1 - \frac{4\pi R^3}{12\sqrt{2}\ r_d^3} \qquad \text{(IV-64)}$$

Recalling that the depleted volume is the same as the bubble volume,

$$r_d = R \sqrt[3]{2} \qquad \text{(IV-65)}$$

and

$$\rho_m = 1 - \frac{1}{6 \sqrt{2} \, \pi} \qquad \text{(IV-66)}$$

Rapid nucleation, therefore, will produce

$$\frac{1}{4 \sqrt{2} \, r_d^3} \left(1 - \frac{1}{6 \sqrt{2} \, \pi} \right) = \frac{5.4446}{r_d^3} \text{ cells} \qquad \text{(IV-67)}$$

per original unit volume of polymer. A typical nucleation radius for the fast regime is 5.08×10^{-4} μ (2×10^{-8} in). In this case, the cell density will be 4.15×10^{22} cells/cm^3 sec (6.8×10^{23} cells/in^3 sec).

For low nucleation rates, the computer model does not take relaxation of the plastic into account, and therefore will over estimate the cell density. This matter could be corrected by incorporating a modulus which changes with time. For these systems, however, cell growth is such a major factor that it would also be necessary to keep track of cell "pirating." This is the phenomena in which large cells draw gas from smaller ones by diffusion. Since the larger cells have lower internal pressures, a concentration gradient is set up between

them and the smaller cells. To account for this, it is necessary to
abandon the assumption that all cells have identically sized diffusion
zones and allow the size of the diffusion zone to vary with cell size and
the local configuration of cells (each having a different diameter). This
introduces a great deal of complication into the program. Making an
intelligent assumption of a "typical" local cell configuration can
be tricky. Once it has been established, the size of the diffusion zones
can be obtained from the condition that the boundary concentrations of
adjacent regions must match. Hopefully, it would be possible to conceive
of a packing configuration so that the diffusion regions could be assumed
spherical, otherwise the calculation would become even more hopelessly
complicated.

Since the foams resulting from the slow nucleation regime will have
large cell sizes and consequently poor quality, a detailed accounting of
them was not considered worth the effort. Instead, the conditions for
which this regime occurs have been mapped in Figure IV-11 and IV-12.

The computer programs is useful for predicting the qualities of
foam in the intermediate nucleation regime. The program is described in
full in Appendix C. Because of the extensive calculation time already
mentioned, the rates of nucleation for various conditions and diffusion
rates were calculated independently, then were coordinated by hand.

The subroutine (or function) which finds the nucleation rate is
PROG. In accordance with the classical nucleation theory discussed
earlier, the change of Gibb's free energy (ΔG) for bubbles of different
sizes is determined. The maximum ΔG is the activation energy which
must be overcome to produce a stable bubble nucleus. The rate of nuclea-

To read Figures IV-11 to IV-13.

The nucleation regime is determined by four variables. To determine if a state is in the fast nucleation regime, pick the graph in accordance with the system's temperature, then find the point corresponding to the surface tension and modulus. The concentration must be above that of the equi-concentration line running through that point. Use the same procedure for slow nucleation, except the concentration must be below that of the equi-concentration line running through that point.
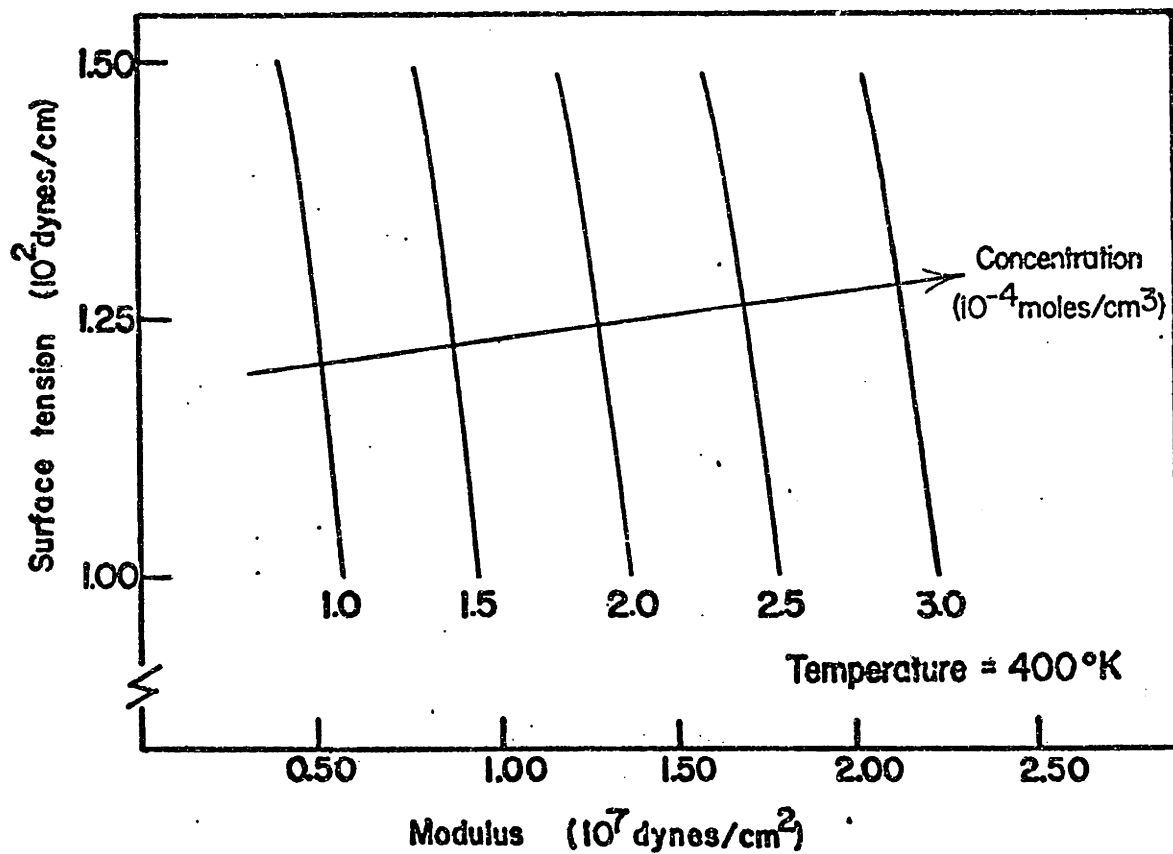
FIGURE IV-11 BOUNDS BETWEEN FAST AND INTERMEDIATE DIFFUSION ZONES

FIGURE IV-12   BOUNDS BETWEEN FAST AND INTERMEDIATE DIFFUSION
ZONES – CONTINUED

FIGURE IV-13   BOUNDS BETWEEN INTERMEDIATE AND SLOW DIFFUSION
ZONES

FIGURE IV-13 BOUNDS BETWEEN INTERMEDIATE
AND SLOW DIFFUSION ZONES

tion follows an Arrehenius relationship. The cell size for which ΔG is a maximum is called the critical radius, and it is assumed that newly nucleated cells are this size. The rate of nucleation depends upon the size of the diffusion zone, the size of the cell (actually the pressure within it), and, of course, the diffusion coefficient. The size of the diffusion zone is calculated from the cell density by assuming that the zones are all the same size and closepacked. A method to calculate the size of the zone is shown in Appendix B. As mentioned before, using diffusion zones which are all the same size predicts cells of only one size. This is acceptable, however, since in this regime, variations in nucleus size are less than 5%. As discussed in Section IV.B.b, the diffusion equation was solved for the conditions that the radial derivitive of the radial derivitive of the concentration distribution at the outside boundary is zero, and that the concentration at the edge of the bubble is

$$C_o = \frac{\text{pressure in bubble}}{K} \tag{IV-68}$$

For the initial condition, the concentration profile shown in Figure IV-9 was used. The sloped region ($r = R$ to r_o) represents the region depleted during nucleation. As an easy and crude approximation, it was assumed to be 1/10 of the outside radius of the depleted zone. Actually, its thickness is .288 X R.

Once tables of diffusion and nucleation rates were obtained, iterations to calculate the final cell density were made by hand. An initial

time step was chosen so that at least 1% of the final number of cells would be produced in subsequent time steps. The later time steps were generally somewhat shorter to gain an accurate estimate of the cell density. The number of cells produced per unit volume during each time step was added until the increase was insignificant. As long as the above procedure was followed, variations in time step did not significantly alter the results.

Graphs of cell density versus critical parameters for this nucleation regime are shown in Figure IV-14, IV-15, IV-16, and IV-17.

Once an estimate has been made of the number of cells nucleated, diffusional and relaxational growth can be predicted.

Diffusional growth stops once pressure equilibrium is attained between the cells and the gas in the surrounding matrix. The size of the cells at this point can be calculated by determining the excess of gas between the initial concentration and the final equilibrium, then dividing by the number of cells per unit volume. If the concentration is in moles, this can be converted to cell volume (or radius) by the ideal gas law. However, because the pressure of the cell (and hence the equilibrium pressure) is dependent on the cell size, the expression for R is a quartic equation:

$$1 = \left[\frac{C_0}{\frac{2\gamma}{R} + \frac{E}{\pi} + 14.T} - \frac{1}{K} \right] \frac{RT \cdot 3}{R^3 4 \cdot \cdot \pi \rho_c} \qquad \text{(IV-69)}$$

This was solved by computer (the program is in Appendix D). The resulting

FIGURE IV-14 CELL DENSITY VS. INITIAL GAS CONCENTRATION

FIGURE IV-15 CELL DENSITY VS. MODULUS

FIGURE IV-16 CELL DENSITY VS. TEMPERATURE

FIGURE IV-17 CELL DENSITY VS. SURFACE TENSION

FIGURE IV-18   CELL RADIUS VS. TEMPERATURE

cell sizes are shown in Figures IV-18 to IV-20.

The above expression can be used to calculate the relaxational growth as well, simply by allowing the modulus to change with time. Graphs of cell size versus time (or modulus) are in Figure IV-22 to Figure IV-25.

This model, as every other, has its limitations. These must be recognized and understood before the model can be used with confidence.

One of the most important limitations has already been discussed at length. For the polymer system described, the critical radius predicted by classical nucleation theory has sub-atomic dimensions. This indicates that a non-classical theory of nucleation must be employed and that perhaps even the concept of nucleation rate is questionable.

If the program is considered despite this flaw or applied to systems whose critical cell size does not fall within this regime, there are other limitations to be realized. One important assumption is that the reaction occurs isothermally. Because of the speed of both nucleation and diffusion, the gas is rapidly decompressed. Since the gas must be reheated, and since the material around the edge of the cell may be cooled (thereby experiencing an increase in modulus), the energy required to foam the plastic is underestimated by the model. Also, the rapid expansion sheds doubt on the expression for Gibb's free energy used in the nucleation theory. The expression does not account for momentum effects, or the energy needed to overcome increases in modulus due to high strain rates. Again, the prediction of the energy needed for nucleation is too low.

In addition to the shortcomings of the nucleation theory, the

FIGURE IV-19 CELL RADIUS VS. MODULUS

FIGURE IV-20 CELL RADIUS VS. SURFACE TENSION

FIGURE IV-21   CELL GROWTH AS A FUNCTION OF INITIAL
GAS CONCENTRATION

FIGURE IV-22 CELL GROWTH VS. INITIAL MODULUS

FIGURE IV-23   CELL GROWTH VS. SURFACE TENSION

FIGURE IV-24 CELL GROWTH VS. TEMPERATURE

theory describing the diffusional growth deviates from nature by not accounting for the change of bubble pressure as the bubble grows. To take this into account would result in a differential equation different from that of Fourier, and one more difficult to solve. The approximation used gives a lower estimate of the size of the cell, since as the bubble grows, the pressure in the cell decreases, allowing more gas to be driven into the cell. Also, diffusion would occur at a faster rate than predicted.

The discrepancies just described are those between the theoretical bases of the model and nature. In addition to these, there are also simplifications introduced to be able to express the theory in a computer program.

As already discussed, the program assumes that the cells reorganize themselves into a close packed configuration. In addition, the model assumes that there are always enough sites to sustain nucleation at the classically predicted rate. As with the quasi-steady assumptions, this will also predict a value of Gibb's free energy that is too low, and thus over estimate the cell density.

V. RESULTS

Temperature, modulus, concentration, solubility, surface energy and diffusion coefficient: all of these play major roles in the growth of cellular foam. To design successful foaming processes, it is important to understand the role of each.

A. Temperature and Modulus

a) Nucleation

Since the energy of mixing is proportional to RT ln X/X_2, high temperatures during nucleation yield a high energy of gas supersaturation. This leads to high densities of small cells, as shown in Figure IV-15. Since the modulus is low when temperature is high, little energy is spent deforming the matrix, and the trend of increasing densities of smaller cells with higher temperatures is intensified (cell density versus modulus for constant temperature is shown in Figure IV-16, for moduli which depend upon temperature, see Figure V-1). It should be noted, however, that increasing temperature also causes an increase in the diffusion coefficient. For the slow and intermediate nucleation rate regimes, higher diffusion rates will hasten cell growth and thus lower density. For foams produced in the laboratory, all of the material was heated from room temperature to above T_g. Thus, the temperature of the matrix is increasing during nucleation and growth. Since the gas concentration and material characteristics remained unchanged while the oven temperature was varied, modulus and surface tension each depended only on

FIGURE V-1 FOAM CHARACTERISTICS FOR MATERIAL WITH
TEMPERATURE-DEPENDENT MODULUS (PART A)

FIGURE V-1 FOAM CHARACTERISTICS FOR MATERIAL WITH
TEMPERATURE-DEPENDENT MODULUS (PART B)

FIGURE V-1 FOAM CHARACTERISTICS FOR MATERIAL WITH
TEMPERATURE-DEPENDENT MODULUS (PART c)

temperature. Thus, nucleation should have begun at the same critical temperature for each sample, regardless of the final temperature. Since nucleation is completed in such a short time, the oven temperature is expected to influence foam formation most during the relaxational growth regime. Inspection of Figure III-7 substantiates this suggestion; the size of the cells increases with oven temperature. Since growth was halted in these systems at 7.5 minutes, the modulus was not zero, but varied with temperature (see Figure V-3). This would lead to cell sizes which increase with higher temperatures. For the intermediate systems analyzed by computer, increasing the diffusion coefficient by half gave increases in cell density of only 10%. Here the effect of the increase of modulus with temperature is much more dramatic.

b.) Diffusional Growth

During diffusional growth, temperature plays its predominant role in changing the diffusion coefficient. High temperature, and thus rapid diffusion is responsible for shorter diffusional growth time. In slowly nucleated systems which have non-uniform cell sizes, high temperature causes larger spread in cell size distribution. In these cases, high temperatures are not desirable during diffusional growth since they lead to larger maximum cell size.

c) Relaxational Growth

In this realm, high temperatures, by causing the modulus to be low, allow bubbles to grow faster and larger. Orientation is destroyed more readily. For foams in the fast and intermediate nucleation regimes, the effects of temperature and modulus during nucleation outweigh their

FIGURE V-2 CELL SIZE VS. TIME (TEMPERATURE-DEPENDENT MODULUS)

FIGURE V-3 MODULUS VS. TEMPERATURE AFTER 7.5 MINUTES

effect during relaxational growth (see Figure V-2).

B.   Initial Concentration

    a) Nucleation

    Concentration plays its most important role during nucleation. With higher supersaturation of gas in the matrix, more energy is available for forming cells and more cells form. Since the residual supersaturation of gas remaining after nucleation is divided among them, a higher cell density means smaller cells. Since the amount of residual gas has little to do with the initial concentration, realizing the initial gas concentration increases the cell density, decreases cell size, and improves material properties.

    b) Diffusional and relaxational growth

    The increase in cell size during the diffusional growth is based on the excess of gas and the cell density. Since the nucleation rate depends quite steeply upon concentration, increasing the initial gas concentration decreases cell size, as shown in Figure IV-21. The dependence of cell size on concentration in laboratory produced foam is shown in Figure III-1.

C.   Surface Energy

    a) Nucleation

    Energy must be invested in new surface when cells are formed. Thus, the number of cells increases as the surface energy coefficient decreases, while their size decreases. See Figure IV-17.

FIGURE V-4 CELL DENSITY VS. SURFACE TENSION

b) Diffusional Growth

The surface tension resists growth of the cell and maintains a pressure difference between the interior and exterior of the cell. Smaller cells have higher internal pressures than larger ones. In the slow regime, which has large bubble size variations, this effect causes the larger ones to attract gas from the smaller cells. Higher surface energy coefficients make this undesirable effect more pronounced.

c) Relaxational Growth

Since the surface tension resists cell growth, it aids the mechanical properties during this period. However, as cells grow larger, the effects of surface energy become less and less significant when compared to volumetric quantities, such as modulus.

VI. CONCLUSIONS

Through the course of this work, the following conclusions have been reached:

(1) A method for producing microcellular foam has been demonstrated. The material produced has tensile strength which is superior to that of conventional foam, and which improves as cell size decreases. However, the method requires long cycle times which eliminate its usefulness as a commercial process.

(2) Classical nucleation theory was applied to a system consisting of a polymer matrix supersaturated with a specified amount of gas to determine the rate of nucleation and ultimate cell density. The amount of gas diffusing to each cell was estimated, and finally the growth of the cell due to the relaxation of the matrix was determined. Although applying classical nucleation theory to polystyrene foams may not be valid, the theory predicts that high nucleation rates result from large drops in free energy during foaming. Initial and final conditions which enhance the free energy drop are favorable for the production of microcellular foam. These are:

* Increasing initial gas concentration.

* Decreasing surface tension.

* Increasing the temperature of the process.

* Decreasing the modulus of the material.

(3) Foam has three stages of development: nucleation, diffusional

growth and growth due to matrix relaxation. Since nucleation will halt once the level of gas supersaturation falls below a critical value, the type of foam produced depends upon the competition between nucleation and diffusion for available gas. When nucleation occurs so rapidly that gas diffusion is insignificant, the cell density will be very high and the amount of gas which can be absorbed by each cell will be small.

If diffusion and nucleation have similar time constants, diffusion will reduce the gas concentration between the cells and ultimately stop nucleation. The foams have intermediate cell densities and larger cells, but the distribution of cell sizes is expected to be fairly narrow.

If nucleation is extremely slow, relaxational growth will occur while nucleation and diffusion are taking place. These foams should have comparatively poor qualities, with low cell densities, large cells, and a wide distribution of cell sizes.

The number of cells nucleated should be as high as possible. To achieve this, nucleation should be completed as quickly as possible. If nucleation is triggered during less favorable conditions, it does not matter if more favorable conditions ensue; large cells have already been nucleated and are growing.

Future Work

There is still much to learn. In addition to developing a commercially feasible process for producing microcellular foam, other future

endeavors are suggested by this work.

The classical theory of homogeneous nucleation theory does not appear to apply to the systems studied. The critical nucleii are predicted to be so small that they are comparable to free volume voids existing in the polymer. Nucleation should be examined with a more detailed understanding of the fluctuations and movements of the polymer chains. Also, the event occurs so rapidly that the equilibrium assumptions should be questioned. The model should account for the drop in the temperature of the material due to the decompression of the gas.

More data is needed to gain a better quantitative knowledge of the effects of various process parameters on the morphology and the strength of the foam produced. Waldman (1980) has already begun work on measuring the impact strength of the foam. Fracture of foam should be studied, probably using the concept of J-integrals. Also, it would be instructive to model the amount of orientation imposed during the formation of a bubble, how much of it is lost before the foam is cooled, and the effects of such orientation on strength.

Finally, this foaming method should be tried with other combinations of polymer and gas and adopted for thermo- and chemosets.

By understanding polymer foams more clearly, they may become important engineering materials, offering improved materials properties and lower densities.

REFERENCES

Becker, R. and Doring, W. (1935), Ann. d. Physik, 24 (5), p. 719.

Benning, Calvin J. (1969), Plastic Foams, Wiley-Interscience, N.Y.

Blander, Milton and Katz, Joseph (1975), "Bubble Nucleation in Liquids," AIChE Journal, 21 (5), p. 833-848.

Cole, Robert (1979), "Boiling Nucleation," Advances in Heat Transfer, 10, p. 85-166.

Cogswell, F.N. (1964), Polymer Eng. and Sci., 12 (1), p.64.

Denbigh, Kenneth George (1968), The Principles of Chemical Equilibrium, 2nd ed., Cambridge Univeristy Press, Cambridge, England. Chapter 8.

Dudek, Annette L. (1979), Effects of Photo-oxidation on t'e Solubility and Transport Properties of Polymers, M.S. Thesis, Case Western Reserve University, May 1979.

Farkas, L. (1927), Z. Physik Chem., 125, p. 236.

Frisch, (1965), "Mechanisms for Fickian Diffusion of Penetrants in Polymers," J. of Polymer Eng. Sci., B. 3, p. 13-16.

Gent., A.N. and Tompkins, D.A. (1969), "Nucleation and Growth of Gas Bubbles in Elastomers," J. Appl. Physics., 40 (6), p. 2520-2525.

Gibbs, Williard, Scientific Papers, 1, date unknown.

Han, C.D., Kim, Y.W., and Malhotra, K.D. (1976), "A Study of Foam Extrusion Using a Chemical Blowing Agent," J. of Appl. Polymer Sci., 20, p. 1583-1595.

Han, C.D., and Villamizar, (1978), "Studies on Structural Foam Processing - The Rhelogy of Foam Extrusion," Polymer Eng. and Sci., July 1978, 18 (9), p. 687-698.

Hansen, Ralph (1962), "Production of Fine Cells in the Extrusion of Foams," SPE J., 18 (1), Jan. 1962, p. 77-82.

Hardenburg, Scott, (1980), Eastman Kodak Co., Rochester, N.Y., personal communication.

Hatsopoulos, George and Keenan, Joseph H. (1965), Principles of General Thermodynamics, especially Chapters 26 and 29., John Wiley & Sons., Inc., N.Y.

Hildebrandt, Francis, (1964), Advanced Calculus for Applications,

Prentice-Hall, Inc., Englewood Cliffs, N.J., p. 155.

Hobbs, S.Y. (1975), "The Application of Structure - Property Studies to Structural Foams," Polymer Eng. and Sci., December 1975, 15 (12),p. 854-862.

Moiseyev, (1960), Expanded Plastics, Macmillan, N.Y.

Reid, R.C., Prausnitz, J.M., and Sherwood, T.K. (1977), The Properties of Gases and Liquids, McGraw-Hill, N.Y., p. 602-627.

Reid, R.C. (1978), "Superheated Liquids...Laboratory Studies and Theory," Chem. Eng. Ed., 12, p. 60-87.

Reiss,R. (1950), J. Chem. Physics, 18 (7), p. 996.

Rohsenow, Warren M. and Hartnett, James P. (1973), Handbook of Heat Transfer, McGraw-Hill, N.Y., p. 4-57 to 4-58.

Russell, Kenneth C. (1980, "Nucleation in Solids," to appear in Nucleation III, A.C. Zettlemoyer, ed., Marcell Decker, N.Y.

Saunders, J.H. and Hansen, R. (1972), "The Mechanism of Foam Formation," in Plastic Foams, K.C. Fritsch and J.H. Saunders, ed., Marcel Dekker, p. 39.

Throne, James (1979), Science and Technology of Polymer Process, Nam P. Suh and Nak-ho Sung, ed., MIT Press, Cambridge, MA, p. 77-131.

Tucker, A.S. and Ward, C.A. (1975), "Critical State of Bubbles in Liquid-Gas Solutions," J. of Appl. Physics, 46 (11), p. 4801-4808.

Volmer, M. (1939), Kinetik der Phasenbildung, Dresden T. Steinkopf.

Waldman, Francis (1980), Massachusetts Institute of Technology, Cambridge, MA., personal communication.

Worthy, Ward (1978), "Versatile Microporous Polymers Developed," C&NE, December 11, 1978, p. 23-24.

Wu, Souheng (1970), "Surface and Interfacial Tensions of Polymer Melts II," J. of Physical Chemistry, 74 (3), p. 634.

Zeldovich, J.F. (1943), "On the Theory of New Phase Formation; Cavitation," Acta Physicochimica U.R.S.S., 18 (1), p. 1-22.

Zettlemoyer, A.C., (ed.) (1969), Nucleation, Marcel Dekker, N.Y., especially Chapters 1, 2 and 5.

Appendix A

SURFACE TENSION OF POLYBUTADIENE AT 120°C

The parachor, P, is a quantity which relates surface tension to molecular volume, V (or, in this case, mer volume) by

$$\gamma = \left(\frac{P}{V}\right)^{1/4} \tag{Ap. A.1}$$

Values for the parachor can be found by adding contributions from each atomic group in the mer. A list of the contributions of various groups of atoms have been published (Reid, 1977). For polybutadiene, the parachor is 145 $\left[\frac{cm^3}{mole} \times \frac{erg}{cm^3}\right]^{1/4}$. The molar volume of 25°C is 60.87 cm^3/mole, and the thermal expansion coefficient, 22 X 10^{-5} /°C. For a 95°C temperature rise, the molecular volume increases to a value of 64.77 ca^3/mole. Using the above formula, the surface tension of 120°C is 25.12 dynes/cm (1.43 X 10^{-4} lb/in).

Appendix B

DETERMINATION OF r_d (OUTR)

It was assumed that each bubble is surrounded by a spherical "diffusion region" (a control volume which gas neither enters nor leaves), and that all the regions are the same size, regardless of the size of the cell within. It was also assumed that the regions formed a close-packed configuration. For a standard unit cube of a close-packed matrix, there is a sphere (radius r_d) at each corner and the center of each face, so

$$4r_d^2 = a^2 \cdot 2 \qquad \text{(Ap. B.1)}$$

$$\sqrt{2}\ r_d = a \qquad \text{(Ap. B.2)}$$

Since there are 4 cells per cube (which has side-length 2a), the cell density is

$$\rho\ \text{cell} = \frac{4}{8a^3} = \frac{1}{2a^3} \qquad \text{(Ap. B.3)}$$

Substituting A for a,

$$\rho \; cell \; = \; \frac{1}{2 \left[\sqrt{2} \right]^3 r_d^3} \; = \; \frac{1}{4 \sqrt{2} \; r_d^3} \qquad \qquad (Ap. \; B.4)$$

$$= \; \frac{1}{5.657 \; r_d^3}$$

In the program, r_d, is called OUTR.

Appendix C

COMPUTER CALCULATION OF CELL SIZE DISTRIBUTION

This appendix describes the computer program designed to calculate the cell size distribution corresponding to specified processing or material parameters (modulus, temperature, surface tension, initial gas concentration, diffusion coefficient, solubility, etc.). The main program is described first, followed by the subroutines. The subroutine scheme is shown in Figure A-C-1, and the program is listed starting on page 134. The program was written in APL on the MIT MULTICS system.

A.   Main Program - CELDIST

1.   Input Section

The first section of the program simply establishes the input parameters, and pre-sets certain incrementing values. The conditions are printed before the distribution calculation is made. Ther version shown increments through modulus and temperature, calculating the cell size distribution for each set of parameters.

2. Nucleation Section

The purpose of the second section is to determine the number of cells nucleated during each time increment. First, however, it determines the concentration at which the concentration at which the rate of nuclea- would be negligible (CRITCON: found by the subroutine CUTCONC), so that a test can be made to see if nucleation will occur (line 45). Secondly, it chooses a time step of a fraction the time it would take to double

Subroutine Scheme

Main Program	1st Sublevel	2nd Sublevel	3rd Sublevel
CELDIST	CUTONC	CRITRAD	
		GIBBS	
		RATE	
	PROG	CRITRAD	
		GIBBS	
		RATE	
	DIFF	LAMDA	
		GASIN	
		AN	STRATE
			SLOPE
	NEWSIZE		
	DONELY	GASIN	
		NEWSIZE	
	CONCEN		

the volume of the matrix. (This is chosen because of the gas-volume condition described previously.) Finally, the number of cells nucleated during that time step is determined. PROG is the function which finds the nucleation rate as well as the critical radius, R and the change of Gibb's free energy, G. The number of cells nucleated is found by multiplying the rate by the length of the time increment (line 84). A count is made (line 75) to be able to keep track of the nucleation groups. (This will be used later to index a matrix containing the pertinent information about each group.)

3. Diffusional Growth Section

The growth of the cells by diffusion is calculated using the solution determined in Chapter IV, Section B.

To determine the growth of the cells by diffusion, each cell was assumed to be in a spherical region across which no gas flows. These regions are assumed to be close-packed, and their radius is calculated by lines 93 and 94. TOTCEL is the total number of cells per cubic thou. From the arguments in Appendix B, the radius of the diffusion sphere, OUTR, is $(1/4 \sqrt{2} \text{ TOTCEL})^{1/3}$. The solution found to the diffusion equation is the sum of a series of partial solutions, each having a different separation constant λ_n, and summing coefficients A_{λ_n} . The details of finding the λ's and the A_λ's and incorporating them all into a summed solution of the flow of gas (M) into the cell is all included in the function (subroutine) DIFF (line 110), which depends on the number of the group and the size of the cell. The codes between lines 93 and 110 establish the concentration gradient surrounding newly nucleated cells.

This gradient is shown in Figure IV-9.   It is divided into 10 segments; those in the depleted region are attributed a zero CONC (line 105) (PRESS/K, the actual concentration at the boundary of the cell will be added to the final solution.) The segment containing the boundary of the depleted zone is slanted between 0 and the initial concentration (so its slope is initial CONC/segment length. Segment length is called CHRI in the program (see line 96). The remaining segments are at the initial concentration. This scheme is facilitated by initially assigning the initial concentration to all of the points in CONSSAVE (the values in CONSAVE represent the concentrations at the end points of each segment – this would make 11. The twelfth value is simply used as a place to store the segment length, CHRI, since it will be needed for later reference. CONSAVE [12] is reassigned in line 101. The loop (LOUP) assigns 0 to points in CONSAVE from the cell radius out until the numbers of segments exceeds that which fit into the depleted region (line 104 and 98).

Once DIFF has established the flux of gas into the cell, NEWSIZE determines the cell size after all this gas has been added. The first part of the section (lines 91 to 117) calculates the diffusional growth of newly nucleated cells, and lines 120 to 132 calculate the growth of previously nucleated cells. For diffusion into groups of cells which are not newly nucleated, DIFF is also used, but this time, the initial concentration is that established during the previous time increment. The LOOP which evaluates growth of these cells extends from lines 120 to 132. The concentration used for calculating the next nucleation rate

is that at the outside edge of the diffusion boundary of the first group of cells. When these calculations are completed a new time is assigned (line 121) and the concentration is re-evaluated. Once nucleation is complete, cell growth is determined by DONELY.

B.   Subroutines

   1. PROG

PROG unites the three functions: CRITRAD, GIBBS and RATE, to establish the rate of nucleation, critical radius, and the change of Gibb's free energy during nucleation. If CRITRAD does not find a critical radius (R = 0), then the computer returns to the main program (where it is aborted again).

   2. CUTCONC

CUTCONC also unites CRITRAD, GIBBS and RATE, but this time increments DOCON from the initial concentration to determine the concentration at which nucleation will become negligible

   3. DIFF

DIFF calculates the flow of gas into the cell (in moles per cell) by calling three other functions, LAMDA, EQCOEF and GASIN. As already mentioned, the flux of gas into the cell is calculated by solving diffusion equation for a spherical region surrounding the cell with insulated boundary conditions, then applying Fourier's equation at the cell boundary. The basis for the insular condition is the assumption that gas will diffuse only to the closest cell, and therefore, there are boundaries between the cells across which flow will not occur. The pro-

gram assumes that this boundary is midway between any two cells, although
this is not true for cells of widely varying radius, where the boundary
is much closer to the smaller cell. If the discrepancy is large enough,
gas will actually leave the smaller cell and go to the larger one.
This is discussed in Chapter V. The subroutine calculates the first 8
values of λ (line 1), then the values of A (line 9 and 10) determines
the flux of gas into the cell (line 13) and the new cell size (line 14).
Finally, it sores the values of λ and A in AAUGH and EQMAT, and the re-
sulting concentration by calling SAVECONC.

4. NEWSIZE

NEWSIZE uses the ideal gas law to approximate the amount of gas
already residing in a cell. To that amount is added the gas which has
flowed into the cell during the last time increment. Finally, the ideal
gas law is used again to determine the final size of the cell.

5. CONCEN

CONCEN determines the concentration at any radius in the diffusant
region. It does this by getting the values of λ and A from EQMAT for
the particular cell group in question, and plugging them into the solu-
tion for concentration. Again, the solution is a series solution, so the
program loops until four terms have been summed.

6. DONELY

DONELY calculates the growth of the cells after nucleation has
ceased. It takes the values of λ and A established during the previous
time increment and determines the growth of each group of cells as time
progresses by taking gas in. This procedure leaves the concentration

distributions intact from one time increment to the next.

7. CRITRAD

CRITRAD searches for the radius at which the change of Gibb's free energy is maximum, called the critical radius. First, it finds the order of magnitude by rising an exponential search, then it changes to a decimal search. To find the order of magnitude, it creates the vector TRYR. Consisting of a list of exponentially increasing numbers (line 2). It then determines the derivitive of the Gibb's free energy change with respect to R at each of the radii listed in TRYR. Line 11 establishes a vector (HOLD) the same length as TRYR, but having a 1 if the derivitive is negative, and a 0 if it is positive (line 11). Line 12 takes the successive sum of the components in HOLD. $(0_1 0_1 0_1 1_1 1_1 1)$ → $(0\ 0\ 0\ 1\ 2\ 3)$. IND is assigned a vector having a 1 only where the vector has a 1 (and 0 elsewhere), line 13. By multiplying IND with TRYR, the radius R is found which is an over approximation to the critical radius. Now, TRYR is reassigned a new vector, this time a list of numbers increasing decimally up to the value R. For the exponential search, this is done by assigning log R to START. Then multiplying a list of numbers from 1 to 10 by 10 raised to (START-1), line 17. (The first term in 17 is 0 because court is 1, and 10 raised to START is R. See Gilman and Rose (1976) for a PL calculation SYNTAX; it calculates from right to left without regard for the type of operation). NUMB is increased by 1 and the calculation is repeated starting from LUPE on line 4. Now, when line 14 is calculated, R is multidigital. Its exponent is stored in START (by rounding up the logarithm), and now the first term in line 17 decreases

the last digit in R by 1, then adds to it an array of numbers from 1 to
10 in the next smallest digit.   This is repeated 8 times for accuracy.

8.   GIBBS

GIBBS simply calculates the change of Gibb's free energy once the
critical radius is determined.   There are three terms D3, D4 and D5; the
deformational energy, the surface energy, and the mixing energy which
are added together.

9.   RATE

RATE is a straightforward calculation of the rate at which cells
form.   The rate equation was discussed earlier, and it was shown that the
rate of nucleation,

$$J = \beta_c S_c N_o Z \exp(-\Delta G/KT)$$

where β_c is the frequency at which gas molecules strike a surface, S_c is
the surface area (calculated in lines 1 and 2), N_o is the number of
possible nucleation sites (6.55×10^{22} sites/in^3) and Z is the Zeldonich
factor (calculated as line 11). ΔG is the change in Gibb's free energy
for a cell of critical size and was calculated by GIBBS.   K is Boltzman's
constant, and T the temperature.

10. LAMDA

LAMDA determines the separation coefficients of the diffusion equa-
tion.   Although there are an infinite number of these constants, only
15 are determined by this calculation.   The order of magnitude of
the first λ is established by letting TRYL equal a list of 1000 numbers

between 0 and 1/log OUTR. This choice of TRYL insures that two roots do not appear in the list, that the root does not occur between 0 and the first value in the list (1/1000 · log OUTR), and that the root is determined with sufficient accuracy. The characteristic equation that λ must satisfy is evaluated by line 15. ONEL must be 1 if the equation is satisfied. To search for λ, ONEL is compared with a vector RONEL (which is ONEL rotated by one element). All intervals over which ONEL changes from less than one to greater than one are tested for slope to see if they are zeros or poles. The zeros are recorded as values for λ. The calculation is repeated for higher values of TRYL (the second set of values from 1/(log OUTR) to 2/(log OUTR) until 15 λ's are obtained.

Due to the extensive search routines and the time inefficiencies of APL, this sub-routine often takes three hours to run on the MIT MULTICS system.

11. NEWEQCO

Only the first part of NEWEQCO, which determines the denomenator of A, is used. The numerator is determined by AN (which must be run after NEWEQCO and writes over many of the values found by the later part of NEWEQCO). It is a fairly straight forward - albeit long - expression of the integration stated for A in Chapter IV, Section B. Lines 7 and 8 are concerned with the possibility that the diffusion zone may be smaller in this time increment than the last. In this event, the CONC distribution is cut off cn the outside.

12. GASIN

GASIN plugs the values for λ and A into the expression for the

derivitive of the concentration at the cell boundary. Multiplying this
by the diffusion coefficient and by $4\pi R^2$ determines the amount of gas
which flows into the cell.

13. AN

AN is another long computation, but this program calls on sub-
routines SLOPE and STRATE to keep things simpler. The program sums the
contribution of the rectangular and triangular parts of the CONC distribu-
tion.

14. SAVECONC

This program simply loops to recalculate the concentrations stored
in CONSAVE. (This could be done with a matrix approach as opposed to
a loop.) The function determining the new concentration is CONCEN
(line 6).

```
      ∇CELDIST[□]∇
    ∇ CELDIST
[1]    MOD←250
[2]    CONSAVE←50 12 ρ 0
[3]    SURFT←2.5E¯6
[4]  CON:CO←CO
[5]  SUR:MOD←MOD+250
[6]    →(MOD>2000)/0
[7]    CO←0.00301
[8]    CONC←CO
[9]    TEMP←390
[10] MODU:TEMP←TEMP+10
[11]   CONC←CO
[12]   →(TEMP>420)/SUR
[13]  ⍴PRINT OUT INPUT PARAMETERS
[14]   ' '
[15]   ' '
[16]   ' '
[17]   ' '
[18]   ' '
[19]   ' '
[20]   '                CELL SIZE DISTRIBUTION CALCULATION'
[21]   ' '
[22]   ' '
[23]   'INPUT PARAMETERS:'
[24]   ' '
[25]   'CONCENTRATION='
[26]   CONC
[27]   'MODULUS, TEMPERATURE, SURFACE TENSION, AND 1/SOLUBILITY='
[28]   MOD
[29]   TEMP
[30]   SURFT
[31]   K
[32]   ' '
[33]   ⍴
[34]   ⍴************************NUCLEATION SECTION********************
[35]   ⍴
[36]   'CALCULATED VALUES:'
[37]   ' '
[38]  ⍴FIRST, FIND THE CONC AT WHICH NUCLEATION WILL
[39]  ⍴   NOT OCCUR.
[40]   'THE CONCENTRATION AT WHICH NUCLEATION WILL NOT OCCUR IS'
[41]   CRITCON←CUTCONC CONC
[42]   CRITCON
[43]  ⍴FIND THE INITAL RATE OF NUCLEATION
[44]   PROG
[45]   →((G÷(1.2218E¯22×TEMP))>85)/CON
[46]  ⍴NOW, CHOOSE A TIME STEP.  LET IT BEDEPENDENT ON THE RATE
[47]  ⍴   SO THAT ONE TENTH OF THE CELLS ARE NUCLEATED DURING
[48]  ⍴   EACH STEP.
[49]   'THE TIME STEP IS'
[50]   →(R=0)/CON
[51]   TIME←(1÷(4.188×(R×J)))×(0.0001×1E¯9÷(R×R))
[52]   →(TIME>1)/TSTOP
[53]   TIME←TIME×1E2
```

```
[54]  BACK;TIME
[55]   RUNTIME←TIME
[56]   ⍝FINALLY, CALCULATE THE CELLS NUCLEATED DURING THAT TIME STEP
[57]   COUNT←0
[58]   TOTCEL←0
[59]   MATRX←2 4 ⍴0
[60]   '  '
[61]   '  '
[62]   '---------START NUCLEATION---------------'
[63]   '  '
[64]   EQMAT←2 2 8 ⍴0
[65]  AGIAN:'  '
[66]   '  '
[67]   'TIME:'
[68]   RUNTIME
[69]   'CONC='
[70]   CONC
[71]   PROG
[72]   'EQUIL CONC='
[73]   EQCONC←PRESS[1]÷K
[74]   EQCONC
[75]   COUNT←COUNT+1
[76]   '  '
[77]   'THE CRITICAL RADIUS IS'
[78]   R
[79]   'THE CHANGE OF GIBBS FREE ENERGY (IN IN-LB) IS'
[80]   G
[81]   'THE RATE OF NUCLEATION IN CELLS/CU.THOU/SEC IS'
[82]   J
[83]   'THE NUMBER OF CELLS NUCLEATED PER CU.THOU IS'
[84]   NO←J×TIME
[85]   NO
[86]   PRESS←PRESS[1]
[87]   ⍝
[88]   ⍝**************************DIFFUSION SECTION*******************
[89]   ⍝
[90]   '  '
[91]   ⍝CALCULATE THE DIFFUSIONAL GROWTH.
[92]   TOTCEL←TOTCEL+NO
[93]   OUTR←(((2*.5)÷⍳OTCEL)×(1÷3))×1E¯3
[94]   →(COUNT≠1)/CHEAT
[95]   DEPR←R×1.259921
[96]   CHR1←(OUTR-R)÷10
[97]   →(OUTR<R)/OUTDONE
[98]   DEPN←⌈(DEPR÷CHR1)
[99]   CONCY←CONC-(PRESS÷K)
[100]  CONSAVE[COUNT; ]←CONCY
[101]  CONSAVE[COUNT;12]←CHR1
[102]  INDX←0
[103]  LOUP:INDX←INDX+1
[104]  →(INDX>DEPN)/GOON
[105]  CONSAVE[COUNT;INDX]←0
[106]  →LOUP
```

```
[107] GOON:'CONSAVE='
[108] CONSAVE[COUNT; ]
[109] →((TIME÷(OUTR*2))<1E4)/NODIF1
[110] M←COUNT DIFF R
[111] →(M<0)/MODU
[112] PROCEED1:
[113] SIZE←TIME NEWSIZE R
[114] ₳
[115] VECTOR←RUNTIME,NO,SIZE,R
[116] MATRX←MATRX,[1]VECTOR
[117] →(COUNT=1)/NEWTIME
[118] ₳
[119] GROUP←0
[120] NEWG:GROUP←GROUP+1
[121] →(GROUP≥COUNT)/NEWTIME
[122] B←GROUP+2
[123] NO←MATRX[B;2]
[124] R←MATRX[B;3]
[125] →((TIME÷(OUTR*2))<1E4)/NODIF1
[126] M←GROUP DIFF R
[127] →(M<0)/MODU
[128] PROCEED2:
[129] SIZE←TIME NEWSIZE R
[130] MATRX[B;3]←SIZE
[131] OUTDONE:→(COUNT=1)/DOVER
[132] →NEWG
[133] DONLY:DONELY EQMAT
[134] →MODU
[135] NEWTIME:RUNTIME←RUNTIME+TIME
[136] MATRX
[137] CONC←CONSAVE[1;11]+EQCONC
[138] 'NEW CONCENTRATION='
[139] CONC
[140] RELCRTCON←CRITCON+EQCONC
[141] →(CONC<CRITCON)/DONLY
[142] →AGIAN
[143] TSTOP:STP←1
[144] TIME←.1
[145] →BACK
[146] NODIF1:M←0
[147] →PROCEED1
[148] NODIF2:M←0
[149] →PROCEED2
[150] CHEAT:CONSAVE[COUNT; ]←CONSAVE[1; ]
[151] →GOON
[152] DOVER:'TIME STEP TOO LARGE.'
      ∨
```

```
        ∇SAVECONC[[]]∇
    ∇  SAVECONC GROUP
[1]     RNO←0
[2]     CHR←(OUTR-R)÷10
[3]     CHANGR←R
[4]   ENCORE:RNO←RNO+1
[5]     →(RNO>11)/GO
[6]     CONSAVE[GROUP;RNO]←CHANGR CONCEN GROUP
[7]     CHANGR←CHANGR+CHR
[8]     →ENCORE
[9]   GO:CONSAVE[GROUP;12]←CHR
    ∇
```

```
        ∇CRITRAD[□]∇
     ∇ R←CONC CRITRAD PARAM
[1]     S←0
[2]     TRTR←1E¯12 1E¯11 1E¯10 1E¯9 1E¯8 1E¯7 1E¯6 1E¯5 1E¯4 1E¯3
[3]     NUMB←1
[4]    LUPE:PRESS←14.7+(SURFT×(2÷TRTR))+(MOD÷3.14159)
[5]     DEFCONC←PRESS÷K
[6]     Q1←(2.7182812⊛(DEFCONC÷CONC))×TEMP×73.61×CONC×(TRTR*2)×12.5666
[7]     DCONC←¯2×SURFT×((TRTR*2)×K)
[8]     Q2←DCONC×(CONC÷DEFCONC)×TEMP×73.61×(TRTR*3)×4.1888
[9]     Q3←(SURFT×TRTR×25.132741)+(14.7+MOD÷3.14159)×((TRTR*2)×4.1888)
[10]    DGIBBS←Q1+Q2+Q3
[11]    HOLD←DGIBBS<0
[12]    HOLD←+\HOLD
[13]    IND←HOLD=1
[14]    R←+/(IND×TRTR)
[15]    →(R=0)/0
[16]    START←⌈(10⊛R)
[17]    TRTR←(R-10*(START-NUMB-1))÷(⍳10)×(10*(START-NUMB))
[18]    NUMB←NUMB+1
[19]    YES←NUMB<10
[20]    →LUPE×YES
     ∇
```

```
        IBBS[□]∇
     ∇ G←CONC GIBBS R
[1]     CONCDEFL←(14.7+(2×SURFT÷R)+(MOD÷3.14159))÷K
[2]     TOTGAS←(R*3)×CONC×4.1888
[3]     D3←((R*3)×(61.757+1.333×MOD))
[4]     D4←(R*2)×SURFT×12.5666
[5]     D5←(⊛(CONCDEFL÷CONC))×TEMP×73.61×TOTGAS
[6]     G←D3+D4+D5
     ∇
```

```
      ∇RATE[⎕]∇
  ∇   J←CONC RATE R
[1]    STRIKE←6.02E23×(CONC÷MSPACE)×DIFCO×1.5
[2]    AREA←12.5664×(R*2)
[3]    DCONC←¯1×(2×SURFT)÷((R*2)×K)
[4]    DDCONC←4×SURFT÷((R*2)×K)
[5]    W2←⍟(CONCDEPL÷CONC)×TEMP×73.61×CONC×R×25.133
[6]    W3←73.61×DCONC×(CONC÷CONCDEPL)×(R*2)×25.133
[7]    W4←(¯4.1888)×((DCONC÷CONCDEPL)*2)×CONC×TEMP×73.61×(R*3)
[8]    W5←DDCONC×(CONC÷CONCDEPL)×TEMP×73.61×(R*3)×4.1888
[9]    W6←(SURFT×25.1333)+R×25.1333×((MOD÷3.14159)+14.7)
[10]   DDGIBBS←W2+W3+W4+W5+W6
[11]   Z1←((-DDGIBBS)÷(TEMP×1.2218E¯22))*.5
[12]   →(G>100×1.2218E¯22×TEMP)/0
[13]   →((G÷(1.2218E¯22×TEMP))>85)/0
[14]   Z3←*(-G÷(1.2218E¯22×TEMP))
[15]   J←Z3×Z1×6.555E22×AREA×STRIKE×1E¯9×2
  ∇
```

```
        ∇PROG[1]
[1]     R←CONC CRITRAD PARAM
[2]     →(R=0)/0
[3]     G←CONC GIBBS R
[4]     →((G÷(1.2218E¯22×TEMP))>85)/NEW
[5]     J←CONC RATE R
[6]     ∇
```

```
        ∇DIFF[□]
    ∇   M←GROUP DIFF R
[1]     LAMB←OUTR LAMDA R
[2]     AVEC←()
[3]     LAMNO←()
[4]     STG←()
[5]     SUM:LAMNO←LAMNO+1
[6]     →(LAMNO>8)/GO
[7]     →(((L*2)×DIFFCO×TIME)>80)/GO
[8]     L←LAMB[LAMNO]
[9]     A←NEWEQCO
[10]    'A='
[11]    A
[12]    AVEC←AVEC,A
[13]    M←R GASIN TIME
[14]    SIG←M+SIG
[15]    →SUM
[16]    GO:AVEC←1↓AVEC
[17]    AAUGH←LAMB,[.5]AVEC
[18]    EQMAT←EQMAT,[1]AAUGH
[19]    SAVECONC GROUP
[20]    M←SIG
    ∇
```

```
      ∇LAMDA[□]∇
   ∇ LAMB←OUTR LAMDA R
[1]    OUTR
[2]    RREF←10*(⌈(10⍟OUTR))
[3]    TRYL←(00.0001÷RREF)×⍳1000
[4]    HOLDL←TRYL
[5]    LAMB←0
[6]   HONE:V2←TRYL×OUTR
[7]    V3←3○(TRYL×R)
[8]    V4←((3○V2)-V2)÷((V2×(3○V2))+1)
[9]    ONEL←V4÷V3
[10]   RONEL←1⌽ONEL
[11]   POLES←(ONEL×RONEL)>‾1000
[12]   LIND←(((ONEL≥1)∧(RONEL≤1))∨((ONEL≤1)∧(RONEL≥1)))∧POLES
[13]   LIND[1000]←0
[14]   PICK←(TRYL[⍒LIND]×(LIND[⍒LIND]))
[15]   STOP←PICK⍳0
[16]   LAMB←LAMB,((STOP-1)↑PICK)
[17]   →((⍴LAMB)>15)/LOUT
[18]   TRYL←(TRYL[1000])+HOLDL
[19]   →HONE
[20]  LOUT:'=LAMDA'
[21]   LAMB←1↓LAMB
[22]   LAMB←15↑LAMB
[23]   LAMB
   ∇
```

```
      ∇GASIN[□]∇
   ∇ M←R GASIN T
[1]    S1←1○(L×R)
[2]    C1←2○(L×R)
[3]    TERM←S1-((3○(L×R))×C1)
[4]    TERM2←C1+((3○(L×R))×S1)
[5]    TPART←AX(*(-(L*2)×DIFFCO×T))
[6]    M←12.566×(R*2)×DIFFCO×TPART×(TERM÷(-L×(R*2)))+(TERM2÷R)
   ∇
```

```
      ∇AN[□]∇
   ∇ AN
[1]    SL1←(1÷CHR)×((SLOPE (CHR+R))-(SLOPE R))
[2]    SL2←(R÷CHR)×((STRATE (CHR÷R))-(STRATE R))
[3]    SLANT←SL1-SL2
[4]    STRAIT←((STRATE OUTR)-(STRATE (CHR+R)))
[5]    A←(SLANT-STRAIT)÷DENOM
   ∇
```

```
         ∇NEWEQCO]ω[[]]∇
      ∇  A←NEWEQCO
[1]      SUMM←()
[2]      NEWSLOPE←()
[3]      TOST←()
[4]      SAVENUM←()
[5]      RNO←()
[6]      OUTR
[7]      HISS←⌊((OUTR-R)÷CONS[12])
[8]      APOUTR←(HISS×CONS[12])+R
[9]      'APPROXIMATION OF OUTR='
[10]     APOUTR
[11]     S1←1⊖(L×R)
[12]     S2←1⊖(L×APOUTR)
[13]     C1←2⊖(L×R)
[14]     C2←2⊖(L×APOUTR)
[15]     T1←3⊖(L×R)
[16]     TERM1←(APOUTR-R)÷2
[17]     TERM2←((C2×S2)-(C1×S1))÷(2×L)
[18]     TE1←(T1*2)×(TERM1+TERM2)
[19]     T2←(TERM1-TERM2)
[20]     T3←T1×((S2*2)-(S1*2))÷(L×2)
[21]     T3←T3×2
[22]     DENOM←(TE1+T2-T3)÷(L*2)
[23]     'DENOM='
[24]     DENOM
[25]     CHR←CONS[12]
[26]     CHANGR←R
[27]  INTEG:RNO←RNO+1
[28]     →(RNO>HISS)/ON
[29]     →(RNO>11)/ON
[30]     CR1←(CHR×(RNO-1))+R
[31]     CR2←(CHR×RNO)+R
[32]     CC←2⊖(L×CR1)
[33]     SC←1⊖(L×CR1)
[34]     CR←2⊖(L×CR2)
[35]     SR←1⊖(L×CR2)
[36]     SLP1A←(-((CR1÷L)*2)×CC)+(((2×CR1)÷(L*3))×SC)+(((2÷(L*4))×CC))
[37]     SLP2A←(((CR1÷L)*2)×SC)+(((2×CR1)÷(L*3))×CC)-((2÷(L*4))×SC)
[38]     SLP1B←(-((CR2÷L)*2)×CR)+(((2×CR2)÷(L*3))×SR)+(((2÷(L*4))×CR))
[39]     SLP2B←(((CR2÷L)*2)×SR)+(((2×CR2)÷(L*3))×CR)-((2÷(L*4))×SR)
[40]     SLOPEPT1←(1÷CHR)×(SLP1A-((T1×SLP2A)))
[41]     SLOPEPT2←(1÷CHR)×(SLP1B-((T1×SLP2B)))
[42]     SLOPEPT←(SLOPEPT2-SLOPEPT1)×(CONS[RNO+1]-CONS[RNO])
[43]     STR1←((CR2÷L)×CR)-(((1÷L)*2)×SR)
[44]     STR2←((CR2÷L)×SR)+(((1÷L)*2)×CR)
[45]     STR3←((CR1÷L)×CC)-(((1÷L)*2)×(1⊖(L×((CHR×(RNO-1))+R))))
[46]     STR4←((CR1÷L)×SC)+(((1÷L)*2)×CC)
[47]     STRAIGHT←(1÷L)×((-(STR1+T1×STR2))+(STR3+T1×STR4))
[48]     →(RNO<2)/EGG
[49]     TOST←TOST+STRAIGHT
[50]  EGG:
[51]     NUM←(SLOPEPT+CONS[RNO]×STRAIGHT)÷DENOM
[52]     SUMM←SUMM+NUM
[53]     CHANGR←CHANGR+CHR
[54]     →INTEG
```

```
      ∇STRATE[□]∇
   ∇  STRAIGHT←STRATE RVAL
[1]    SR←1○(RVALxL)
[2]    CR←2○(RVALxL)
[3]    STR1←((RVAL÷L)xCR)-(((1÷L)*2)xSR)
[4]    STR2←((RVAL÷L)xSR)+(((1÷L)*2)xCR)
[5]    STRAIGHT←(1÷L)x(STR1+T1xSTR2)
   ∇
```

```
      ∇SLOPE[□]∇
   ∇  SLOPEPT←SLOPE RVAL
[1]    SR←1○(LxRVAL)
[2]    CR←2○(LxRVAL)
[3]    SLP1←(-((RVAL÷L)*2)xCR)+(((2xRVAL)÷(L*3))xSR)+((2÷(L*4))xCR)
[4]    SLP2←(((RVAL÷L)*2)xSR)+(((2xRVAL)÷(L*3))xCR)-((2÷(L*4))xSR)
[5]    SLOPEPT←SLP1-(T1xSLP2)
   ∇
```

```
      ∇NEWSIZE[[]]∇
    ∇ SIZE←T NEWSIZE R
[1]     M←M×T
[2]     MO←(PRESS×4.1888×(R*3))÷(73.61×TEMP)
[3]     MOLEG←MO+M
[4]     NEWVOL←(MOLEG×73.61×TEMP)÷PRESS
[5]     SIZE←(NEWVOL÷4.1888)*.3333333
    ∇
```

```
      ∇DONELY[[]]
    ∇ DONELY EQMAT
[1]     RUNSTEP←1÷((L*2)×DIFFCO)
[2]     KOUNT←0
[3]   REPEAT:RUNTIME←RUNTIME+RUNSTEP
[4]     MATRX
[5]     ' '
[6]     'TIME:'
[7]     KOUNT←KOUNT+1
[8]     RUNTIME
[9]     →(KOUNT>85)/0
[10]    →((RUNTIME×(L*2)×DIFFCO)>85)/0
[11]    GROUP←0
[12]  ROWL:GROUP←GROUP+1
[13]    →(GROUP>COUNT)/REPEAT
[14]    LAMNO←0
[15]    B←GROUP+2
[16]    R←MATRX[B;3]
[17]    M←0
[18]  LAM:LAMNO←LAMNO+1
[19]    →(LAMNO>8)/GRR
[20]    L←EQMAT[B;1;LAMNO]
[21]    A←EQMAT[B;2;LAMNO]
[22]    →((RUNTIME×(L*2)×DIFFCO)>85)/0
[23]    SAQ←R GASIN RUNTIME
[24]    M←SAQ+M
[25]    →LAM
[26]  GRR:→(M<0)/ROWL
[27]    MATRX[B;3]←RUNSTEP NEWSIZE R
[28]    →ROWL
    ∇
```

```
        ∇CONCEN[□]∇
    ∇  NEWCON←CHOSER CONCEN GROUP
[1]     AD←0
[2]     NEWCON←0
[3]   SOL:AD←AD+1
[4]     →(AD≥2)/0
[5]     B←GROUP+2
[6]     L←EQMAT[B;1;AD]
[7]     A←EQMAT[B;2;AD]
[8]     NEWC←TIME C CHOSER
[9]     NEWCON←NEWCON+NEWC
[10]    →SOL
    ∇
```

Appendix D

CELL SIZE AS A FUNCTION OF MODULUS
(FINAL)

This program calculates cell size as a function of modulus (or as a function of time as the material relates).

```
      ∇FINAL[□]∇
   ∇ FINAL
[1]   MOD←600
[2]  PETE:MOD←MOD-100
[3]   →(MOD<0)/0
[4]   TRR←5E⁻8+(TRx\1000)
[5]   UPPER←73.61×TEMP÷(4.1888×TOTCEL×(TRR*3))
[6]   LOWER←(CONC÷((SURFT×2÷TRR)+(MOD÷3.14159)+14.7))-(1÷187000)
[7]   SCAN←LOWER×UPPER×1E⁻9
[8]   BR←SCAN<1
[9]   DO←BR\1
[10]  MOD,TRR[DO]
[11]  →PETE
   ∇
```

Appendix E

DIFFUSION AND SOLUBILITY COEFFICIENTS

FOR N_2 GAS IN POLYSTYRENE

The diffusion of gas into the plastic was measured by weighing samples of plastic before and after they had resided in the pressure chamber with 2.4×10^7 dynes/cm^2 N_2 gas for varying lengths of time. A Mettler analytic balance (Model H I5) was used. The change of weight due to absorption of the gas was measurable with at least two significant digits (the smallest change was 0.0078 gms for a piece which originally weigh.ed 9.6529 gms [after 6 hours N_2 at 2.4×10^7 esults of this are shown in Figure Ap. E.1. Both the solubility of the N_2 in polystyrene and the diffusion coefficient can be calculated from this data.

A. Solubility

Assuming Henry's law holds,

$$K = \frac{0.0016 \text{ gms } N_2}{\text{gm PS}} \cdot \frac{1}{2.4 \times 10^7 \text{ dynes/cm}^2} \qquad \text{(Ap. E.1)}$$

$$= 6.67 \times 10^{-11} \frac{\text{gms } N_2}{\text{gms PS}} / \text{dynes/cm}^2$$

B. Diffusion

For a sheet of polymer suddenly immersed in a penetrant vapor at a higher pressure, the amount of penetrant entering the sheet after short
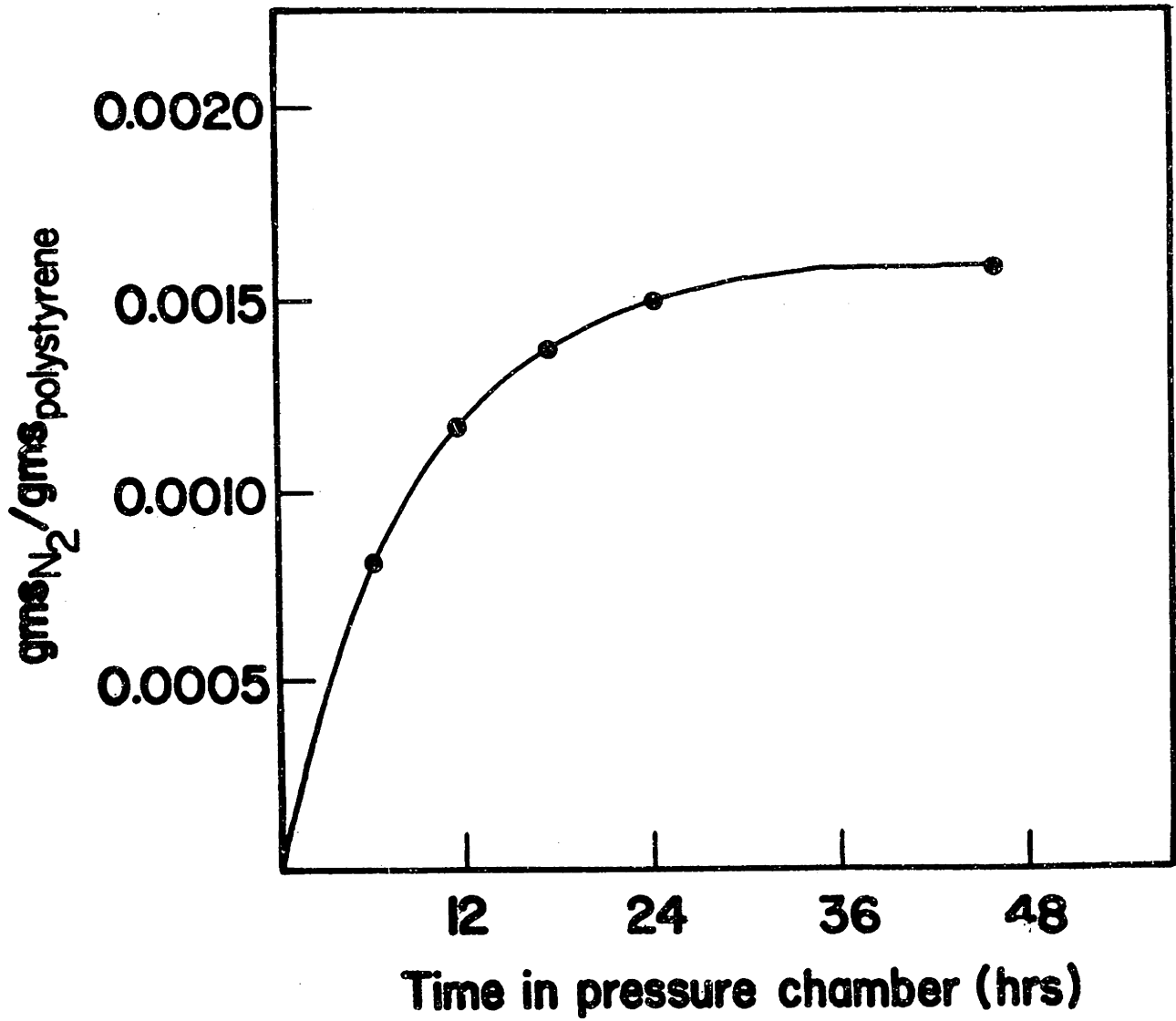
FIGURE Ap.E.1 GAS CONCENTRATION Vs. TIME

time periods is M(t), where

$$\frac{M(t)}{M(\infty)} \; = \; \frac{4}{<} \; \sqrt{\frac{\mathcal{D}t}{\pi}} \qquad\qquad \text{(Dudek, 1979)} \qquad\qquad \text{(Ap. E.2)}$$

$M(\infty)$ is the amount of penetrant which enters the sheet at $t = \infty$, $\mathcal{D}$ is the diffusion coefficient, and a suitably short time step is one for which

$$\frac{\sqrt{\mathcal{D}t}}{L} \; <\sim \; \frac{1}{4} \; \cdot \qquad\qquad \text{(Ap. E.3)}$$

This expression is based on the assumption that the sheet was at equilibrium before immersion, that the diffusion coefficient is not dependent upon concentration, and that equilibrium is reached instantly at the surfaces of the sheet.

The diffusion coefficient is thus calculated from the data in Figure A-E-1 to be $3.67 \times 10^{-10} \, cm^2/sec$.

Appendix F

PRODUCTION OF MICROCELLULAR FOAM BY EXTRUSION

The number of cells nucleated should be as high as possible. To achieve this, nucleation should be completed as quickly as possible. If nucleation is triggered during less favorable conditions, it does not matter if more favorable conditions ensue; large cells have already been nucleated and are growing.

F.N. Cogswell (1972) has evaluated the pressure drop which occurs across a die for making extruded rod. He assumed that the drop from the reservoir behind the die to the atmosphere could be evaluated by summing three components: the pressure reduction due to shear in the die, the drop due to extensional flow through the die, and the drop incurred by the material exiting the reservoir. If a die is assumed which has lands of zero length, then the first two components are zero, and the pressure can be calculated as the material exits the reservoir. This is a function of the distance from the die opening. To find out whether or not microcellular foam can be produced by extrusion, it is important to know how quickly the pressure drops. In Appendix III of his paper, Cogswell sums over an infinite series of control volumes to find the net drop from $T = \infty$ to $T = 0$. The ratio of the drop across one differential element to the total drop can be evaluated as

$$\frac{dP}{P_t} = \frac{(\psi + 1)(1 - \omega^{\psi})}{4\psi} + \frac{(1 - \omega)(\psi + 1)}{4} \qquad \text{(Ap. F.1)}$$

where P is pressure, P is the total pressure drop, ψ = melt, index (usually denoted as n), and $\omega = \left(\dfrac{d\Omega}{d\Omega + \Omega}\right)^3$. The flow of the material moving from the rese.oir has a coni-cyclindrical geometry, and Ω is the radius of the involved flow (it is a function of T). By requiring that the pressure drop be a minimum, Cogswell was able to calculate the shape of the region to be

$$\Omega = \Omega_0 \ \left(\frac{T}{\psi} + 1\right)^{\frac{2}{3\psi - 1}} \tag{Ap. F.2}$$

where Ω_0 is the radius of the die, and

$$\psi = \left(\frac{\tau}{\upsilon}\right)^{1/2} \frac{\Omega_0 \sqrt{2}}{3\psi_{-1}} \tag{Ap. F.3}$$

where τ and υ are apparent viscosities (usually termed λ and n, respectively).

If the flow were Newtonian (which occurs for polystyrene melts at shear rates below 10^{-5}/sec), Eq. (Ap. F. 1) reduces to

$$\frac{dP}{P_t} = 1 - \omega.$$

Substituting for ω,

$$\frac{dP}{P_t} = 1 - \left(\frac{\sqrt{\frac{2}{3}} \ T + \Omega_0}{\sqrt{\frac{2}{3}} \ (T + dT) + \Omega_0}\right) \tag{Ap. F.4}$$

If the pressure drop is to occur in less than 10^{-3} sec, and if the material is moving toward the die at 0.05 in/sec, then this equation must predict that the pressure drop be negligible 5×10^{-5} in before the die. Using an Ω_0 of 0.025 in and setting $dH = 1 \times 10^{-5}$ in (using a dH of 5×10^{-6} in only affects the 3rd significant digit), integration (done on a TI 59 programmable calculator) shows that the pressure has already dropped 99.5%. Thus, pre-nucleation has occurred. The distance over which the drop is significant is of the same order as the die radius. Reducing the die opening to 5×10^{-5} is unfeasible. To make the orifice a useful size, the melt velocity must be higher. For instance, an orifice with a 0.01 in radius requires a melt velocity of 10 in/sec. This is conceivable, but larger die openings demand prohibitive extrudate speeds.

If the fluid is not assumed to be Newtonian, examination of Eq. (Ap. F.1) shows that the only way to make $\frac{dP}{P_t}$ decrease rapidly with increasing T is to make χ increase rapidly with T. This depends upon the behavior of the function

$$\Phi = \frac{1}{1 + \frac{\Gamma}{T}} = \frac{T}{T + \psi}$$

Figure (Ap. F.2) shows that Γ should be small as possible. But

$$\Gamma = \frac{dT}{3\psi_{-1}}$$

so ψ should be as large as possible. For most viscoelastic polymers,

however ψ is less than 1. Thus, the Newtonian fluid already analyzed is the best case. That analysis showed that it would be difficult to extrude all but very narrow profiles of microcellular foam. The only hope for larger shapes is to find a polymer-gas combination which has a very low diffusion coefficient, even at extrusion temperatures. In this way, the limit of 10^{-3} sec might be extended.

Appendix G

INTEGRATION TO FIND VISCOUS ENERGY TERM

```
        ∇INTEGRATE[□]∇
     ∇  INTEGRATE
[1]     R←ι1000
[2]     R←R×.001
[3]     CUBE←1+((1÷R)*3)
[4]     A←(CUBE*(¯2÷3))-1
[5]     B←(CUBE*(¯5÷3))÷R
[6]     TERM1←A×B×8×3.14159
[7]     C←(CUBE*(1÷3))-1
[8]     D←(CUBE*(¯2÷3))÷R
[9]     TERM2←C×D×8×3.14159
[10]    SUM←(+/TERM1)+(+/TERM2)
[11]    SUM←SUM×.001
     ∇
```